Biochimica et Biophysica Acta 1853 (2015) 3279–3293

Contents lists available at ScienceDirect

Biochimica et Biophysica Acta

journal homepage: www.elsevier.com/locate/bbamcr

DPF2 regulates OCT4 protein level and nuclear distribution

Chao Liu [a,b,*], Dijuan Zhang [a], Yuxian Shen [c], Xiaofang Tao [c], Lihua Liu [d], Yongwang Zhong [b], Shengyun Fang [b,**]

[a] Department of Histology and Embryology, Institute of Stem Cell and Tissue Engineering, School of Basic Medical Sciences, Anhui Medical University, Hefei, Anhui 230032 China
[b] Center for Biomedical Engineering and Technology (BioMET), University of Maryland, Baltimore, MD 21201 USA
[c] School of Basic Medical Sciences, Institute of Biopharmaceuticals, Anhui Medical University, Hefei, Anhui 230032 China
[d] Institute of Clinical Pharmacology, Anhui Medical University, Hefei, Anhui 230032, China

ARTICLE INFO

Article history:
Received 29 May 2015
Received in revised form 28 August 2015
Accepted 21 September 2015
Available online 28 September 2015

Keywords:
OCT4
DPF2
PHD finger
E3
Ubiquitination

ABSTRACT

The amount of transcription factor OCT4 is strictly regulated. A tight regulation of OCT4 levels is crucial for mammalian embryonic development and oncogenesis. However, the mechanisms underlying regulation of OCT4 protein expression and nuclear distribution are largely unknown. Here, we report that DPF2, a plant homeodomain (PHD) finger protein, is upregulated during H9 cell differentiation induced by retinoic acid. Endogenous interaction between DPF2 and OCT4 in P19 cells was revealed by an immunoprecipitation assay. GST-pull down assay proved that OCT4 protein in H9 cells and recombinant OCT4 can precipitate with DPF2 *in vitro*. *In vitro* ubiquitination assay demonstrated DPF2 might serve as an E3 ligase. Knock down of *dpf2* using siRNA increased OCT4 protein level and stability in P19 cells. *DPF2* siRNAs also up-regulates OCT4 but not NANOG in H9 cells. However, RA fails to downregulates OCT4 protein level in cells infected by lenitviruses containing *DPF2* siRNA. Moreover, overexpression of both DPF2 and OCT4 in 293 cells proved the DPF2–OCT4 interaction. DPF2 but not PHD2 mutant DPF2 enhanced ubiquitination and degradation of OCT4 in 293 cells co-expressed DPF2 and OCT4. Both wild type DPF2 and PHD2 mutant DPF2 redistributes nuclear OCT4 without affecting DPF2–OCT4 interaction. Further analysis indicated that DPF2 decreases monomeric and mono-ubiquitinated OCT4, assembles poly-ubiquitin chains on OCT4 mainly through Ub–K48 linkage. These findings contribute to an understanding of how OCT4 protein level and nuclear distribution is regulated by its associated protein.

1. Introduction

OCT4 plays crucial roles in maintaining stem cell pluripotency [1–3]. A critical amount of OCT4 is required to sustain embryonic stem cell (ESC) self-renewal and multilineage differentiation capacity [4]. OCT4 is required for generating induced pluripotent stem cells (iPSCs) [5–7]. OCT4 alone is sufficient to generate iPSCs with the aid of small molecules [8,9]. Moreover, OCT4 also plays roles in oncogenesis and may be a potential target for drug therapy of cancer [10–13]. Spatially, OCT4 subnuclear distribution is related to oncogenesis [14,15]. Recent report also showed that OCT4 nucleocytoplasmic dynamics is involved in cell reprogramming and self-renewal of ESCs [16]. In addition, nuclear localization of OCT4 is required for its transactivating activity [17]. Therefore, understanding regulation of OCT4 protein level and intracellular localization may contribute to manipulating OCT4 relevant function and further application.

The ubiquitin (Ub) proteasome system (UPS) is a proteolytic system that regulates protein levels through ubiquitination of its targeted proteins [18,19]. Ubiquitination is a process whereby a small protein, Ub, conjugates its target protein. Mono-ubiquitination occurs through isopeptide bond between the ε-amino group of the lysine (Lys, K) side chain in target protein and the C-terminal glycine (Gly76) residue on Ub, which is achieved through enzymatic cascade activation by E1 (Ub-activating), E2 (Ub-conjugating), and E3 (Ub-ligase) enzymes. The addition of one or more Ub moieties to the first Ub on the target substrates results in di- or poly-ubiquitination [20]. Poly-ubiquitination, instead of mono-ubiquitination, is targeted for proteasomal degradation [21]. UPS thus plays crucial roles in many cellular processes [18], including maintaining pluripotency of stem cells and determining developmental potency of various adult stem cells, through substrate ubiquitination [22]. Recent report indicated that RNF2, an E3, interacts with OCT4 and functions in maintaining stem cell pluripotency [23]. WWP2, another E3, also interacts with OCT4 and regulates OCT4 protein level in human ESCs [24]. While fusion of a single Ub to OCT4 inactivates its transcriptional activity [25], poly-ubiquitination of OCT4 decreases its level [24]. Specifically, K48-linked poly-Ub chains instead of K63-linked

Abbreviations: ESC, embryonic stem cell; iPSC, induced pluripotent stem cell; PHD, plant homeodomain; Ub, ubiquitin; UPS, ubiquitin proteasome system; E3, ubiquitin ligase; RING, really interesting new gene; GST, glutathione S-transferase; RA, retinoic acid; WT, wild type; IP, Immunoprecipitation; IB, immunoblotting; IF, immunofluorescence; siRNA, small interfering RNA; CHX, cycloheximide

* Correspondence to: C. Liu, Department of Histology and Embryology, 69 Meishan Road, Anhui Medical University, Hefei, Anhui, 230032 China.
** Corresponding author.
E-mail addresses: chaol1974@ahmu.edu.cn (C. Liu), sfang@umaryland.edu (S. Fang).

http://dx.doi.org/10.1016/j.bbamcr.2015.09.029
0167-4889/

poly-Ub chains are considered to be a proteasomal degradation signal [18,19]. In UPS, E3s interact directly with substrate proteins and thus determine the substrate levels [18]. E3s also play crucial roles in translocation of the related substrates [26,27]. Two main types of E3s, homologous to the E6AP carboxyl terminus (HECT) and really interesting new gene (RING) finger families of E3s, have been identified [28,29]. HECT domain receives Ub from the E2 through a thiol linkage to a conserved Cysteine and transfers it to substrate. The RING finger marks the vast majority of E3s that play crucial roles in protein degradation and chelate also two $Zn2^{+}$ ions through a conserved set of cysteines and histidines arranged in a Cysteine-3-Histidine-Cysteine-4(C3HC4) pattern [28,29].

DPF2, also named ubi–d4/requiem (REQU), interacts with OCT4 or a protein complex containing OCT4 *in vivo* [30–32]. It contains double plant homeodomain (PHD) fingers and is involved in cell apoptosis [33,34] and also noncanonical NF-kappaB transcriptional activation and its associated oncogenic activity [35]. PHD fingers are zinc-binding motifs that function in DNA binding, chromatin organization and protein–protein interaction [36,37]. However, the exact function of PHD fingers remains elusive. Typical PHD fingers contain a Cysteine-4-Histidine-Cysteine-3(C4HC3) consensus that coordinates two $Zn2^{+}$ ions in a crossbrace topology [38], which is similar with RING fingers [28]. Therefore, PHD finger is considered as one subgroup of RING-related E3s [28]. Indeed, more and more studies discovered that PHD finger proteins function in ubiquitination and degradation of target proteins [39–44], suggesting PHD finger proteins might have shared an E3 activity. We therefore want to check if DPF2 directly interacts with and functions in OCT4 stability and intracellular localization.

In this study, we report that all-trans retinoic acid (RA) treatment leads to down-regulation of OCT4 protein accompanied by up-regulation of DPF2 in H9 cells. DPF2 interacts with OCT4 and serves as an E3 ligase. *dpf2* siRNA increased OCT4 protein level and stability in P19 cells. *DPF2* siRNA also up-regulates expression of OCT4 but not NANOG in H9 cells. However, RA induced differentiation downregulates OCT4 protein level in cells infected by lenitviruses containing control siRNA but not *DPF2* siRNA. Overexpression of DPF2 changes OCT4 subnuclear distribution and increases OCT4 ubiquitination and degradation, and all of these processes depend on the second PHD finger of DPF2. Further analysis indicated that DPF2 decreases monomeric and mono-ubiquitinated OCT4, assembles poly-ubiquitin chains on OCT4 mainly through Ub–K48 linkage.

2. Materials and methods

2.1. Plasmids

The OCT4 plasmid previously described was provided as a gift from Dr. Yun Qiu [6]. The wild-type (WT) DPF2 cDNA was constructed by subcloning a PCR product amplified using primers 5′- CGGAATTCCCATGGAAGATGGCGGCTGTGGTGGAG-3′ and 5′-A CGCGTCGACCAAGAGGAGTTCTGGTTCTGGTAGA-3′ from the pCMV-SPORT6-DPF2 (Open Biosystems, Huntsville, AL) vector and was then cloned into pGEX-5X-1 and pEGFP-N1 vectors via EcoRI/SalI sites. Wild type RNF2 cDNA was amplified by PCR using primers 5′- CGGGATCCCGATGGCAATGTCTCAGGCTGTGCAGAC-3′ and 5′-ACGCGTCGACCGTTTGTGCTCCTTTGTAGGTGCGTAA-3′ from the pDNR-LIB-RNF2 (Open Biosystems, Huntsville, AL) vector and was then inserted into the pGEX-5X-1 vector via the BamHI/SalI sites. pFLAG–CMV–6C–DPF2 was created by excising DPF2 via EcoRI/Sal sites from pEGFP–N1–DPF2 and cloned into the pFLAG–CMV–6C vector. The following point mutations in the gene were introduced using site-directed mutagenesis (Stratagene, La Jolla, CA): a PHD2 mutant DPF2, DPF2 (M), was created using primers 5′-GATCGTGGCTACGCCATGTACGCGTTAACCCCGTCCATG-3′ and 5′-CATGGACGGGGTTAACGCGTACATGGCGTAGCCACGATC- 3′. A 6His-tagged Ub, a lysine null mutant Ub, and a single-lysine-containing mutant Ub were provided as kind gifts from Dr. Yun Qiu. Plasmids encoding FLAG-tagged Ub and HA-tagged Ub were provided as kind gifts from Dr. Yihong Ye. A pET28a-OCT4 plasmid was provided as a kind gift from Dr. Ying-jie Wang.

2.2. Cell culture

P19 cell was cultured as previously described [45]. HeLa and 293 culturing was previously described, respectively [46,47]. Briefly, cells were maintained in Dulbecco's modified Eagle's medium supplemented with 10% foetal bovine serum, 50 units/ml penicillin, 50 μg/ml streptomycin and glutamine under 5% CO_2 in a humidified incubator. Cells were transfected with plasmid DNA by using calcium phosphate precipitation or Lipofectamine 2000 (Invitrogen, Carlsbad, CA). Human ESC line, H9, was maintained on Matrigel (BD Bioscience, Bedford, MA) in mTeSR medium (Stem Cell Technologies, Vancouver, BC, Canada), as previously described [48,49].

2.3. GST-pull down assay

Glutathione S-transferase (GST) fusions were expressed in log phase *Escherichia coli* BL-21 (DE3) (Novagen, Madison, WI) that were grown overnight at room temperature and induced with 0.1 mM isopropyl-1-thio-β-D-galactopyranoside for 1 h. Bacterial pellets were resuspended in sonication buffer (50 mM Tris, pH 7.4, 1 mM EDTA, 1% Triton X-100, 5 mM DTT, 2 mM phenylmethylsulfonyl fluoride) and lysed by probe sonication, using 4 ml of sonication buffer per 100 ml of bacterial culture. The sonicated lysate was clarified by centrifugation at 4 °C for 15 min at 14,000 rpm, aliquoted, and stored at −70 °C. The GST fusion proteins were purified with glutathione-Sepharose beads. His-tagged human OCT4 was expressed in *Escherichia coli* BL-21 and purified using Ni-NTA agarose (QIAGEN, Hilden, Germany) as described previously [50]. H9 cells were treated with MG132 (Calbiochem) at 20 μM for 4 h and lysed in NP-40 lysis buffer (150 mM NaCl, 10 mM Tris/HCl, pH 7.5, 1 mM EDTA, 1 mM EGTA, 1 mM phenylmethylsulfonyl fluoride, 0.2% NP-40). GST-DPF2 and/or GST-RNF2 immobilized on glutathione-Sepharose beads were incubated with H9 cell lysates or recombinant His-tagged OCT4 overnight at 4 °C. After washing with NP-40 lysis buffer, bead-associated proteins were immunoblotted for OCT4. IB was performed following the previously published protocol [51].

2.4. Immunoprecipitation (IP) and immunoblotting (IB)

Immunoprecipitation under native condition was performed as previously described [51]. Briefly, cells were harvested 18–20 h after transfection and lysed in RIPA buffer (50 mM Tris/HCl, PH 8.0, 150 mM NaCl, 1% Nonidet P-40, 0.5% sodium deoxycholate, 0.1% SDS, protease inhibitor cocktail, and 1 mM phenylmethylsulfonyl fluoride) with or without 20 μM MG132. Lysates were incubated with 2–3 μg of primary antibody and 40 μl of protein A (Zymed) or Protein G (Roche Diagnostics, Indianapolis, USA) Agarose overnight at 4 °C. Beads were then washed three times in wash buffer containing 50 mM TrisHCl (pH 7.5), 100 mM NaCl, and 0.5% Triton X-100 before processing for IB as previously described [51]. For immunoprecipitation (IP) under denatured condition, 10% of the harvested cells were lysed with RIPA lysis buffer and kept for input. The other cells were lysed with buffer containing 1% SDS, 15 U/ml DNAse, 5 mM EDTA, 10 mM DTT, heated for 5 min at 95 °C, and then diluted with 9 volumes of RIPA lysis buffer. After incubation on ice for 5 min, the lysates were processed for IP followed by IB assay as previously described [51]. Antibodies used for IB are as follows: rabbit anti-DPF2 (1:5000, Lifespan Bioscience, Seattle, WA, USA), monoclonal rabbit anti-OCT4 (1:3000, Cell Signaling Technology, Danvers, MA, USA), rabbit anti-DPF2 (1:500, Proteintech), rabbit anti-BIP (1:1000, Cell Signaling Technology, Danvers, MA, USA), mouse anti-VCP (1:5000), rabbit anti-GAPDH (1:5000), mouse anti-OCT4 (1:1000,

Santa Cruz Biotechnologies, Santa Cruz, CA, USA), mouse β-actin (1:5000, Sigma, St. Louis, MO, USA), anti-FLAG–HRP (1:1000, Sigma, St. Louis, MO, USA), mouse anti-Ub (1:500–1:2000, Santa Cruz Biotechnologies, Santa Cruz, CA, USA), mouse anti-GST (1:10,000, Proteintech), and rabbit anti-NANOG (1:1000, abcam).

2.5. Fluorescence and immunofluorescence (IF) assay

H9 cells were cultured on Matrigel coated coverslips. The other cells were cultured on coverslips. Transfection was performed with the indicated plasmids using Lipofectamine 2000 or calcium phosphate. Cells were fixed in 4% paraformaldehyde, washed with 1× phosphate-buffered saline (PBS), and blocked for 60 min with 0.1% BSA in 1× PBS containing 0.1% saponin. GFP-tagged proteins in 293 cells were visualized under a fluorescence microscope 16 h after transfection. For FLAG-tagged proteins, transfected cells were labelled using a Cy3-conjugated anti-FLAG (1:500, Sigma, St. Louis, MO) antibody. Transfected OCT4 in 293 cells and HeLa cells were labelled with a rabbit anti-OCT4 antibody followed by incubation with an Alexa Flour-488 (1:500) anti-rabbit antibody. For P19 and H9 cells, endogenous DPF2 and OCT4 were labelled using rabbit anti-DPF2 (1:100, Proteintech) and mouse anti-OCT4 (1:1000, Santa Cruz Biotechnologies, Santa Cruz, CA) antibodies followed by incubation with Alexa Fluor-488 anti-mouse (1:500) and Alexa Fluor-594 anti-rabbit (1:500) antibodies. Staining was performed as previously described [51]. A Zeiss Axiovert 200 M inverted fluorescent microscope, an Olympus IX73 inverted fluorescent microscope and a NIKON Eclipse 80i fluorescent microscope was used for visualization.

2.6. dpf2 siRNA assay

Double-stranded oligonucleotides (GenePharma,Shanghai, China) were designed against three separate regions of mouse *dpf2* cDNA. The sequences of these duplexes are: sense 5′-GCC CAG AGC AAU UGU UAU ATT-3′ and antisense 5′-UAU AAC AAU UGC UCU GGG CTT-3′ for *dpf2 siRNA* # 237; sense 5′-GCU UUC UUU CCC AUC GAU UTT-3′ and antisense 5′-AAU CGA UGG GAA AGA AAG CTT-3′ for *dpf2 siRNA#370*, sense 5′-GCG AGU UUC CUG UUA GCA ATT-3′ and antisense 5′-UUG CUA ACA GGA AAC UCG CTT-3′ for *dpf2 siRNA* # 525. Meanwhile, oligonucleotide targeting against mouse *gapdh* : sense 5′-CAC UCA AGA UUG UCA GCA ATT-3′ and antisense 5′-UUG CUG ACA AUC UUG AGU GAG-3′ served as the positive control, whereas an irrelevant oligonucleotide: sense 5′-UUC UCC GAA CGU GUC ACG UTT-3′ and antisense 5′-ACG UGA CAC GUU CGG AGA ATT-3′ served as the negative control (nc). P19 cells were transfected with mouse siRNAs using lipofectamine 2000 (Invitrogen, Carlsbad, CA, USA).The transfection was performed when cells grew to reach 40–50% confluence as previously described [52]. At 12 h posttransfection, change the culture medium with fresh complete medium. Cells were harvested 72 h after transfection followed by further analysis.

2.7. Lentiviral-vector mediated DPF2 siRNA

A lentivirus-mediated method to establish stable *DPF2* siRNA H9 cell lines was modified according to a previously protocol [53]. Briefly, H9 cells were incubated in mTeSR supplemented with 10 mM Y-27632 at 37 °C for 1 h. Then the cells were dissociated with accutase (Millipore) at 37 °C for 5 min. After washing with mTeSR, the cells were transfer to a 15 mL tube and centrifugated at 500 rpm/min at RT. Then the cells were resuspended in 1 mL mTeSR supplemented with 10 μl of concentrated GFP-expressing lentivirus containing *DPF2* siRNAs (LV-*DPF2* siRNA #25,540, #25,541 and #25,542) (Genechem, Shanghai, China) and incubated at 37 °C for 1 h. Finally, the cell suspension supplemented with 10 mM Y-27,632 was replated on Matrigel-coated 6-well plates and placed gently into incubator. Change medium with mTeSR daily for 5 days. Then apply selection drug puromycin at 10 μg/mL in mTeSR, change medium daily and select for 2 weeks. The stable H9 cell lines were cryopreserved in liquid nitrogen after 3 passages. For transient lentivirus infection of H9 cells, no puromycin selection was performed and a nontargeting siRNA (Genechem, Shanghai, China) was used as a control. The detail information of design of the DPF2 siRNAs is shown in Supplementary Table 1.

2.8. Cycloheximide chase (CHX) assay

Cycloheximide chase experiments were performed as previously described [51]. Briefly, 24 h after transfection, 293 cells were incubated for the indicated times with 100 μg/ml cycloheximide and processed for IB with the indicated antibodies. P19 cells were also incubated for the indicated times with 100 μg/ml cycloheximide 48 h after dpf2 siRNA transfection.

2.9. In vivo ubiquitination assay

For endogenous OCT4 ubiquitination, H9 cells maintained on Matrigel in mTeSR medium were treated with 20 μM MG132 for 6 h. Cells were then subjected to denatured IP using control anti-goat antibodies and anti-OCT4 antibodies to disrupt proteins that may associate with OCT4, followed by IB for indicated proteins.

For ubiquitination of ectopic OCT4, cells were transfected with plasmids encoding OCT4 with or without plasmids encoding HA–Ub, along with or without wild-type (WT) FLAG–DPF2. After 16 h, cells were treated with 20 μM MG132 for 6 h. Cells were then lysed with RIPA buffer containing 5 mM N-ethylmaleimide (NEM), 20 μM MG132, and lastly, 1% SDS, 15 U/ml DNAse, 5 mM EDTA, 10 mM DTT were added to denature proteins. Lysates were diluted in RIPA buffer with a final concentration of 0.1% SDS and used for IP with an OCT4 antibody followed by IB for the indicated proteins.

2.10. H9 cell differentiation induced by all-trans retinoic acid (RA)

H9 cell differentiation induced by all-trans retinoic acid (RA, Sigma) was performed according to our previous protocol [48]. H9 cells grew to reach 60–70% confluence were seeded in 6-well plates pre-coated with Matrigel and maintained in mTeSR medium. The next day (d1), cells were treated with all-trans retinoic acid (RA, Sigma) at 10 μM in fresh mTeSR medium. For a 5-day induction, culture medium was refreshed with mTeSR medium containing 10 μM every day. At d6, the H9 cells were lysed and the lysates were subjected to IB. For a 29-day induction, mTeSR1 medium contain 10 μM RA were replaced every other day. Untreated H9 cells (d0) and cells treated for 5, 9, 14, 19 days, denoted as d5, d9, d14 and d19, were harvested and stored at −80 °C. At d29, all cells were lysed and the lysates were subject to IB for indicated proteins. For differentiation of H9 cells infected by lentiviruses, the cells were subjected to RA treatment for 0, 1, 3 days and harvested at different time points for following IB assay.

2.11. Cytoplasmic and nuclear fraction assay

Cytoplasmic and nuclear fraction was performed according to previous protocol [27]. Cells were harvested, rinsed with phosphate-buffered saline, and pelleted. The cells were then suspended in 5 volumes of cold HB buffer (10 mM Tris, pH 7.9, 1.5 mM MgCl2, 10 mM KCl, protease inhibitor cocktail) and allowed to swell on ice for 15 min, after which Triton X-100 was added to a final concentration of 0.2%. After vortexing for 5 s, the homogenate was spun for 10 min at 1000 g. The supernatant, containing the cytoplasmic fraction, was transferred to a fresh tube, and the salt concentration was adjusted to 200 mM with 5 M NaCl. The crude nuclear pellet was suspended in RIPA-lysis buffer containing 1% Triton X-100 and 10% glycerol, and vortexed vigorously at 4 °C for

30 min. The homogenate was centrifuged for 15 min at 20,000 g. Nuclear and cytoplasmic factions were analysed by IB as described.

2.12. In vitro ubiquitination assay

Using the rabbit reticulocyte lysate (RRL) (Promega, untreated, Madison, Wisconsin, USA) as a source of E1 and E2, the ubiquitination assay of GST–DPF2 was performed as described previously [54]. Briefly, the reaction mixture (150 μl) containing 40 mM Tris–HCl, pH 7.5, 5 mM MgCl2, 2 mM ATP, 2 mM dithiothreitol (DTT), 300 ng/μl ubiquitin (Sigma, St. Louis, Missouri, USA), 25 μM MG132, 5 μl rabbit reticulocyte lysate (Promega, Madison, Wisconsin, USA) and 600 ng GST or GST–DPF2 was incubated at 30 °C for 3 h. Anti-OCT4 immunoprecipitates obtained from H9 cell lysates were used as substrates for *in vitro* ubiquitination assay according to a protocol described previously [55]. The precipitates were washed five times with lysis buffer, once with ubiquitination buffer (40 mM Tris–HCl, 5 mM MgCl2, 2 mM ATP, 2 mM DTT) and subjected to *in vitro* ubiquitination. Finally, all samples were eluted with SDS-sample buffer, resolved by 8% SDS-PAGE, transferred to nitrocellulose membranes and subjected to IB with anti-OCT4, anti-Ub and anti-GST antibodies.

3. Results

3.1. Different expression of DPF2 during early and late stage of H9 cell differentiation induced by RA

RA induces stem cell differentiation and represses OCT4 expression in stem cells [56]. To follow the fate of DPF2 during human ESC differentiation, we treated H9 cells with RA for up to 29 days. Undifferentiated H9 cell clusters were composed of densely packed monolayer cells with clear rims (Fig. 1A). A 5-day culture led to the merging of clumps without differentiation (Fig. 1B). After a treatment for 20 h with RA, cells became flatter, increased in size, and the rims were lost (Fig. 1C). Derived cells proliferated faster than H9 cells and assumed various morphologies (Fig. 1D). Neural tube-like structures were found in clumps after RA induction for 14 days (Fig. 1F), and neuronal precursor cells were found at day 19 of RA induction (Fig. 1G). Results of IB assay indicated that DPF2 exhibits an initial down-regulation followed by up-regulation (Fig. 1I). Notably, OCT4 protein was down-regulated significantly after a 5-day RA induction (Fig. 1I). Additionally, the disappearance of OCT4 was accompanied by increased expression of DPF2 (Fig. 1I and J), which is consistent with that 293 cells and HeLa cells expressed more DPF2 as compared to undifferentiated H9 cells (Fig. S1).

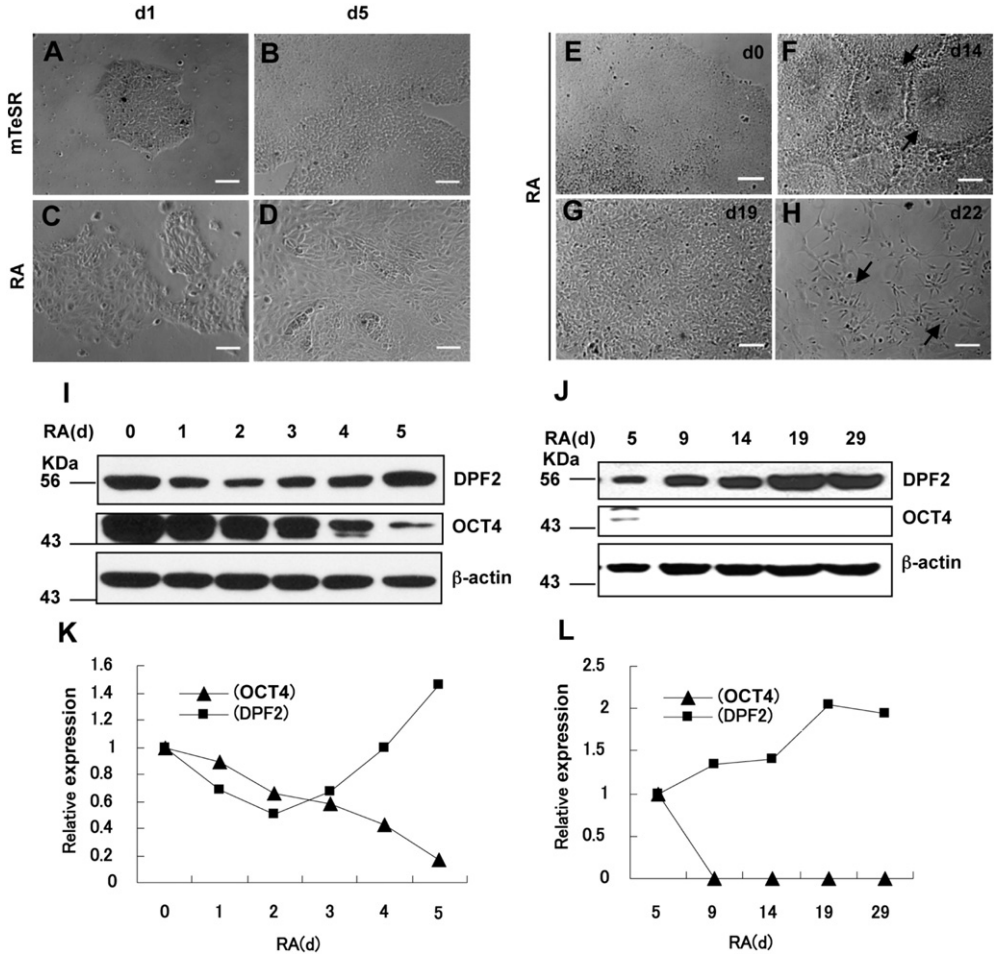

Fig. 1. Differential expression of DPF2 during H9 cell differentiation induced by RA. A–D, H9 cells maintained on Matrigel in mTeSR supplemented with (C and D) or without (A and B) RA for 1 day and 5 days, respectively. Bar = 50 μm. E–H, H9 cells were maintained on Matrigel in mTeSR medium for 4 days (E). Neural tube like structures (arrows, F) formed after 14 days of RA induction. A clump of crowded neural precursor cells after 19 days of RA induction (G). Scattered neural precursor cells (arrows, H) were also identified after 22 days of RA induction. Bar = 50 μm. I and J, The H9 and H9 derived cells were harvested at various time points and subjected to IB for indicated proteins. β-actin was used as a loading control. Medium containing RA was changed every day during the 5-day RA induction, or changed every other day during the 29-day RA induction. K and L, quantitative analysis of relative expression of OCT4 and DPF2 during the 5-day (K) RA induction and the 29-day (L) RA induction, respectively.

These results suggest that DPF2 may play roles in human ESC differentiation.

3.2. DPF2 interacts with OCT4 in vitro and in vivo

We next want to examine if DPF2 co-localizes with OCT4 in H9 cells. MG132 was also used in study of OCT4 protein subcellular distribution [57]. Therefore, we performed IF assay for checking localization of DPF2 and OCT4 in the presence of MG132. Undifferentiated H9 cells maintained in mTeSR medium supplemented with 20 μm MG132 were fixed and subjected to an IF assay. Colocalization of DPF2 (Fig. 2A, D and E, red) and OCT4 (Fig. 2B, D and E, green) was found in nuclei of H9 cells (Fig. 2D and E, arrows). Moreover, DPF2 and OCT4 co-localized with some of the DNA signals that were shown by DAPI staining (Fig. 2C and E, arrows). To examine the interaction between DPF2 and OCT4 *in vitro*, we generated GST–DPF2 and GST–RNF2 fusion proteins to be used in GST-pull down assays. Here, RNF2, an OCT4-interacting RING finger E3, was used as a positive control [23,58]. Both GST–RNF2 and GST–DPF2 were found to copurify with OCT4, with GST–DPF2 interacting more efficiently with OCT4 (Fig. 2F).To further address endogenous DPF2–OCT4 interaction in P19 cells, P19 cells were subjected IF assay with anti-DPF2 and anti-OCT4 antibodies. Colocalization of

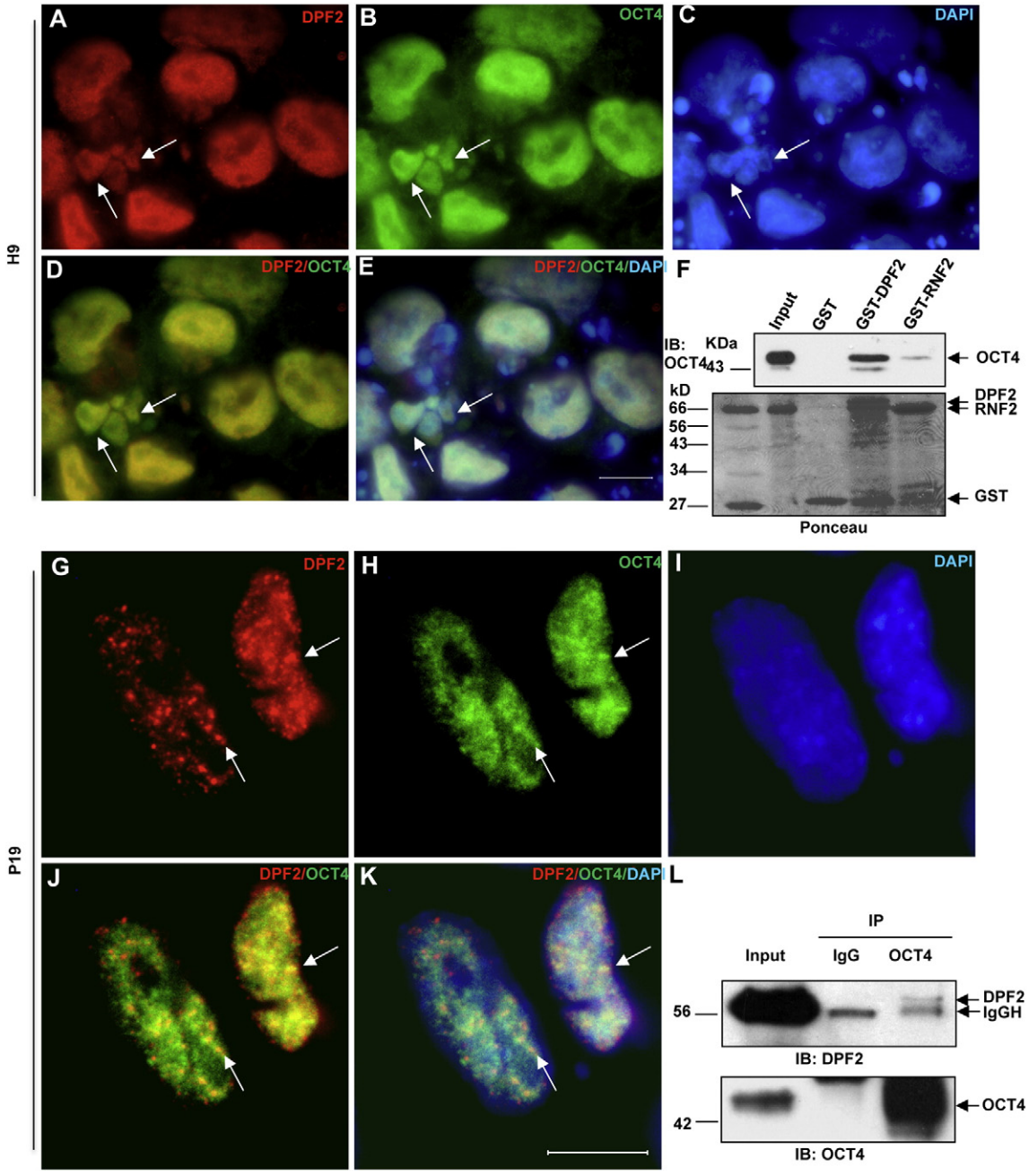

Fig. 2. Interaction between DPF2 and OCT4 *in vivo* and *in vitro*. A–E, H9 cells maintained on Matrigel coated coverslips were fixed and subjected to IF assay using anti-DPF2 (red, A, D and E) and anti-OCT4 (B, D and E, green) antibodies. Nuclei were counterstained by DAPI (blue, C and E). Bar = 10 μm. F, GST, GST-tagged human recombinant DPF2 and RNF2 proteins were incubated with H9 cell lysates and precipitated by glutathione-Sepharose 4B beads, followed by an IB assay with anti-OCT4 antibody (upper panel). Ponceau staining of the PVDF membrane indicates expression of GST and GST-fusion proteins (lower panel). G–K, P19 cells maintained on coverslips were subject to IF assay using anti-DPF2 (G, J and K, red) and anti-OCT4 (H, J and K, green) antibodies. Colocalization of OCT4 and DPF2 was indicated by arrows (G, H, J and K). Nuclei were counterstained by DAPI (blue, I and K). Bar = 10 mm. L, P19 cells were treated with MG132 for 6 h. Then the cells were harvested and the lysates were subjected to IP assay with anti-OCT4 antibody followed by IB for indicated proteins. IP assay with IgG was used as a control. IgGH, IgG heavy chain.

DPF2 (Fig. 2G, J and K, red) and OCT4 (Fig. 2H, J and K, green) was also found in nuclei of P19 cells (Fig. 2J and K, arrows). However, compared with the diffusive distribution of DPF2 and OCT4 in H9 cell nuclei, a punctate distribution pattern of DPF2 and OCT4 in P19 cells was identified.

Next, to prove DPF2–OCT4 interaction using biochemistry method, P19 cells treated by MG132 for 6 h were harvested and subjected to IP using control IgG and anti-OCT4 antibody, respectively, and followed by IB for the indicated proteins. Results also showed that endogenous DPF2 coprecipitated with OCT4 in P19 cells (Fig. 2L). We wonder if DPF2 interacts with ectopic OCT4 in somatic cells. We use enhanced green fluorescent protein (EGFP) as a tag for monitoring intracellular localization of DPF2. Meanwhile, EGFP was used as a negative control, and EGFP-tagged RNF2, RNF2–EGFP, was used as a positive control. Both DPF2–EGFP and RNF2–EGFP expressed mainly in nuclei of 293 cells (Fig. S2A–I). When coexpressed with OCT4, both DPF2–EGFP and RNF2–EGFP showed a colocalization with ectopic OCT4 in double-positive 293 cell nuclei (Fig. S2J–Q, arrows).

These results suggest that DPF2 may serve as an OCT4-associated protein.

3.3. In vitro ubiquitination of OCT4 by DPF2

To demonstrate DPF2 interacts with OCT4 directly, we performed GST-pull down assay using recombinant GST-tagged human DPF2 as a bait protein, His-tagged human OCT4 as a source of prey protein, and recombinant GST as a control. GST–DPF2 but not GST was capable of

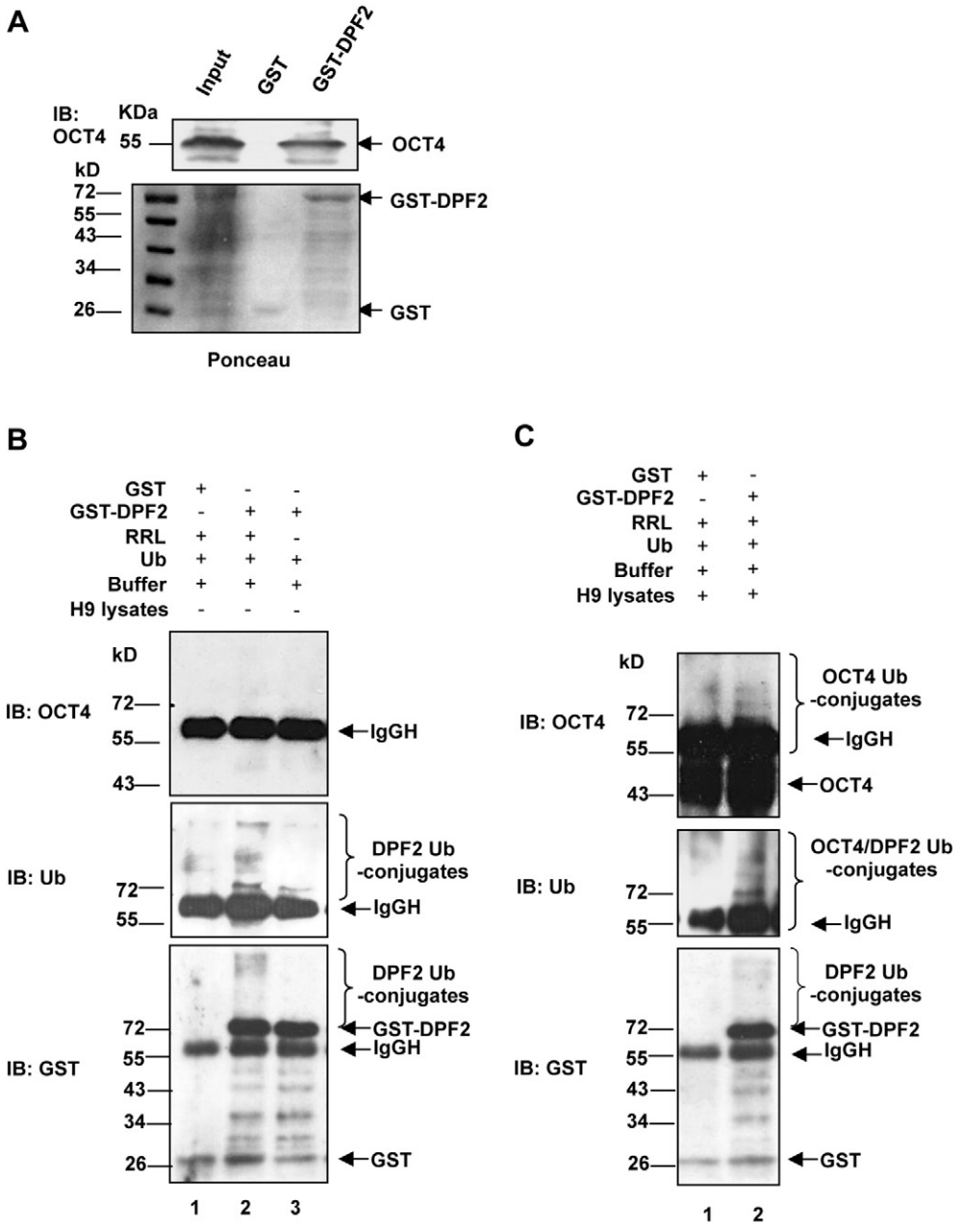

Fig. 3. *In vitro* ubiquitination of OCT4 by DPF2. A, His-tagged human Oct4 was expressed in *Escherichia coli* BL-21 and purified using Ni-NTA agarose. Glutathione S-transferase (GST) fusions were expressed in *Escherichia coli* BL-21 and immobilized on glutathione-Sepharose beads. GST–DPF2 immobilized on glutathione-Sepharose beads were incubated with recombinant His-OCT4 and subjected to IB with anti-OCT4 antibody. Ponceau staining of the PVDF membrane indicates expression of GST and GST–DPF2. B and C, Protein G-Sepharose-bound OCT4 protein was immunopurified from H9 cell lysates. The anti-OCT4 antibody conjugated protein G was used as a control. The immunoprecipitates were subjected to *in vitro* ubiquitination reactions for 2 h through use of RRL and recombinant GST or GST-tagged human DPF2. Then the products of the *in vitro* ubiquitination assay were eluted with SDS-sample buffer, resolved by 8% SDS-PAGE, and immunoblotted with anti-OCT4 (top panel), anti-Ub (middle pannel) and then with anti-GST (bottom panel) antibodies.

pulling down His–OCT4 (Fig. 3A), indicating DPF2 associates with OCT4 directly *in vitro*. We next performed *in vitro* ubiquitination assay using rabbit reticulocyte lysate (RRL) as a source of E1 and E2 and anti-OCT4 immunoprecipitates obtained from H9 cell lysates as substrates. The anti-OCT4 antibody conjugated protein G was incubated with or without H9 cell lysates over night at 4 °C and was subjected to following *in vitro* ubiquitination assay. No ubiquitinated OCT4 was detected (Fig. 3B, top panel, lane 1–3) without the presence of OCT4 precipitates. When compared to GST (Fig. 3B, bottom panel, lane 1), GST–DPF2 formed more ubiquitinated DPF2 species that were recognized by both anti-Ub (Fig. 3B, middle panel, lane 2) and anti-GST (Fig. 3B, bottom panel, lane 2) antibodies. However, ubiquitinated GST-DPF2 was almost lost in the absence of RRL(Fig. 3B, lane 3). With the presence of OCT4 precipitates, more ubiquitinated OCT4 species, which were recognized by both anti-OCT4 (Fig. 3C, top panel, lane 2) and anti-Ub (Fig. 3C, middle panel, lane 2) antibodies, were induced by GST–DPF2 as compared to GST (Fig. 3C, bottom panel, lane 1).

These results suggest that DPF2 might act as an E3 ligase for OCT4.

3.4. Upregulation of OCT4 by dpf2/DPF2 siRNA affects RA induced H9 cell differentiation

Currently, role of DPF2–OCT4 interaction in cell biology is not clear. Therefore, we examined effect of *DPF2*-knockdown on OCT4 expression in P19 cells and H9 cells, respectively, using *dpf2*/*DPF2* siRNAs (Fig. 4). The effect of *dpf2* siRNAs on DPF2 expression was checked first in P19 cells. As expected, negative control (nc) siRNA failed to affect DPF2 expression, while positive control, *gapdh* siRNA, decreased GAPDH expression significantly. The *dpf2* siRNAs showed significant effects on DPF2 expression (Fig. 4A). In P19 cells, #370 *dpf2* siRNA was found more efficient as compared to the other *dpf2* siRNAs. Moreover, *dpf2* siRNA increased expression of OCT4 when compared with *nc* and *gapdh* siRNAs (Fig. 4A). CHX chase time assay was performed at indicated time points using P19 cells transfected by oligonucleotides of nc, *gapdh* and #370 *dpf2* siRNAs, respectively. IB assay result showed that #370 *dpf2* siRNA increased stability of OCT4 (Fig. 4B). Quantitative analysis of the data suggests a significant increase of OCT4 stability by #370 *dpf2* siRNA as compared to *nc* and *gapdh* siRNAs (Fig. 4C).

For H9 cells, stable lines of H9 cells infected by lentiviruses containing oligonucleotides of human *DPF2* siRNAs (#25,540, #25,541 and #25,542) were generated (Fig. 4D). The lentiviruses carrying #25,540 *DPF2* siRNA led to a significant silence of *DPF2* gene as compared to the other *DPF2* siRNAs (Fig. 4E, lane 2). By cytoplasmic and nuclear fraction assay, we found that *DPF2* siRNA induces up-regulation of OCT4 but not NANOG in both cytoplasm and nuclei, with nuclear OCT4 increased more efficiently (Fig. 4F, lane 3 and 4). Especially, while expression of OCT4 was upregulated together with DPF2 down-regulation significantly, NANOG level is reduced in knockdown cells, suggesting a specific up-regulation of OCT4 by *DPF2* siRNA (Fig. 4E and F). It is currently unknown whether down-regulation of OCT4 by DPF2 is involved in hESC differentiation. We thus performed RA-induced differentiation of H9 cells infected transiently by lentiviruses containing control siRNA and different doses (2 μl and 10 μl) of *DPF2* siRNA. Results of IB assay proved knockdown of DPF2 by transient expression of #25540 *DPF2* siRNA, which shows a well dose-effect relationship (Fig. 4G, middle panel, lane 4–6 and lane 7–9). Interestingly, RA treatment downregulated OCT4 in the cells treated by the control siRNA (Fig. 4G, top panel, lane 1–3) but not the *DPF2* siRNA (Fig. 4G, top panel, lane 4–6 and lane 7–9).

These results suggest that *DPF2* may regulate OCT4 protein level *in vivo*, *which is involved in RA induced H9 cell differentiation.*

3.5. Ubiquitination of ectopic OCT4 by overexpressed DPF2

It has been reported that ubiquitin proteasome system plays role in degradation of OCT4 [24,25]. Previously, we also found ubiquitinated OCT4 species, especially high-molecular-weight ubiquitinated OCT4 species, in H9 cells by denature-IP using anti-OCT4 antibody (see Fig. 1, in ref. [59]). To determine whether DPF2 plays role in OCT4 ubiquitination, 293 cells were cotransfected with EGFP, DPF2–EGFP plasmids along with OCT4 plasmids. At 18 h after the transfection, the cells were treated with 20 μM MG132 for 6 h, followed by IP with an anti-OCT4 antibody. Results of IB assay showed that ubiquitinated OCT4 species were recognized by both anti-Ub and anti-OCT4 antibodies, and DPF2–EGFP (Fig. 5A and B, lane 4) induced more poly-ubiquitinated OCT4 species than EGFP (Fig. 5A and B, lane 3). Moreover, DPF2–EGFP but not EGFP precipitated with OCT4, suggesting DPF2 interacts with OCT4 in the 293 cells (Fig. 5C), which is consistent with the colocalization of DPF2–EGFP and OCT4 in Fig. S2J–M.

Because DPF2–EGFP is a C-terminal fusion protein, in which EGFP-tag has a molecular weight of ~30 KDa and might interfere normal localization of DPF2. We thus constructed a plasmid encoding an N-terminal fusion protein of DPF2, FLAG–DPF2, for investigating role of DPF2 in OCT4 ubiquitination. We cotransfected 293 cells with wild type FLAG–DPF2, FLAG–DPF2 (WT) plasmid, along with OCT4 plasmid with (Fig. 5E) or without (Fig. 5D) the presence of HA–Ub plasmid. At 18 h after the transfection, the cells were treated with MG132 for 6 h and subjected to IP using anti-OCT4 or anti-FLAG antibodies. The results of following IB assay indicated that FLAG–DPF2 precipitated with OCT4 (Fig. 5D and E, upper panels, lane 4) and OCT4 precipitated with FLAG–DPF2 (Fig. 5F, lower panel, lane 4).To exclude non-specific binding of OCT4 with FLAG antibody, HeLa cells were cotransfected with plasmids encoding OCT4 and FLAG–DPF2. Then the cells were subjected to IF assay with indicated antibodies (Fig. 5G, a–d). While the cells double positive for OCT4 and FLAG–DPF2 were shown (Fig. 5G, a–d, arrows), cells positive only for OCT4 were also detected (Fig. 5G, a–d, arrowheads), which suggests that OCT4 does not bind FLAG antibody. Further IF assay in 293 cells coexpressed DPF2–EGFP and OCT4 also revealed cells double positive for EGFP and OCT4 (Fig. 5H–J, arrows) and a cells positive only for EGFP (Fig. 5H–J, arrowheads), suggesting DPF2–EGFP does not bind to OCT4. Finally, FLAG–DPF2 increased ubiquitination of OCT4 (Fig. 5D and E, lower panels, lane 4), as compared to FLAG–Vector (Fig. 5D and E, lower panels, lane 3). To examine if OCT4 is indeed ubiquitinated, HeLa cells cotransfected with plasmids encoding FLAG–DPF2 (WT) and OCT4 along with HA–Ub were subjected to IF assay with indicated antibodies. Well colocalization of OCT4 and HA–Ub was detected in aggregate-like structures (Fig. 5K–M, arrows), suggesting that ectopic OCT4 is modified by HA–Ub in 293 cells. These results suggest that overexpression of DPF2 interacts with and promotes ubiquitination of ectopic OCT4 in 293 cells.

3.6. PHD2 finger-dependent ubiquitination and degradation of ectopic OCT4 by DPF2

DPF2 has double PHD fingers in its C-terminal (Fig. 6A). Because PHD finger has E3 activity that plays role in ubiquitination of substrate proteins, we therefore want to investigate if ubiquitination of OCT4 by DPF2 is related to the PHD fingers. We first made a homology analysis for PHD fingers from DPF2 and other proteins showing E3 activity (Fig. 6B). For DPF2, while PHD1 has a homology score of 28%, PHD2 has a score of 39% (Fig. 6C). We next focused on possible role of PHD2 in OCT4 ubiquitination. We constructed a plasmid encoding mutant form of DPF2, FLAG–DPF2 (M), in which the structure of PHD2 was disrupted by mutation in the Histidine 353 and Cysteine 356 of the C4HC3 consensus (Fig. 6D).

To directly assess the effect of PHD2 on OCT4 degradation, we cotransfected 293 cells with FLAG–Vector(V), FLAG–DPF2 (WT) and FLAG–DPF2 (M) plasmids along with OCT4 plasmid in 293 cells. Cells were subject to CHX chase at 24 h after the transfection. Wild-type, but not PHD2 mutant form of DPF2 enhanced OCT4 degradation (Fig. 6E and F). As an E3, DPF2 likely facilitates OCT4 degradation by promoting its ubiquitination, which depends on the PHD2 domain. We next

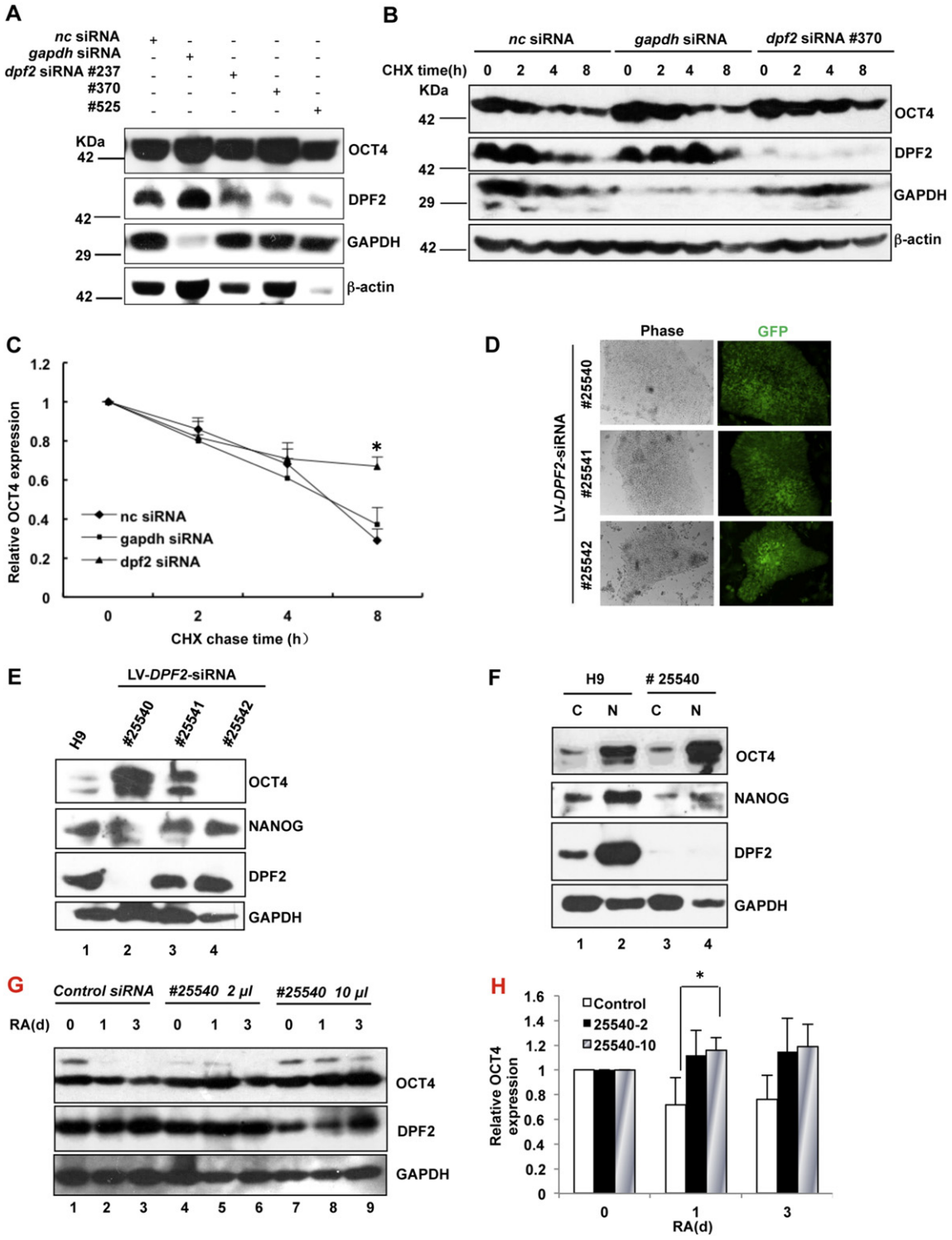

Fig. 4. Upregulation of OCT4 protein level by *DPF2* siRNA affects H9 differentiation induced by RA. A, IB assay for indicated proteins using P19 cells transfected by oligonucleotides of *nc*, *gapdh* and *dpf2* siRNAs (#237, #370 and #525), respectively. nc, negative control. B, Cyclohexmide chase time assay was performed at indicated time points using P19 cells transfected by oligonucleotides of nc *gapdh* and #370 *dpf2* siRNAs, respectively. IB assay was performed for indicated proteins. C, quantitative analysis of data of chase time assay. *, $P < 0.05$ compared to *nc* and *gapdh* siRNA, by independent sample T-test using SPSS 17.0 software. Error bars represent standard error of three-independent experiments. D, phase and fluorescence micrographs of H9 stable cell lines infected by lentiviruses containing *DPF2* siRNAs (#25540, #25541 and #255421). E, H9 cells and H9 stable cell lines with DPF2 knockdown were subjected to IB assay for indicated proteins. F, H9 cells and #25540 H9 stable cell line were subject to cytoplasmic (C) and nuclear (N) fraction assay, followed by IB for indicated proteins. G, H9 cells infected by lentiviruses containing *DPF2* siRNA #25540 were subjected to RA induced differentiation for 0, 1, 3 days and harvested at the different time points for following IB assay with indicated antibodies. A lentivirus-based non-targeting siRNA was used as a control. H, Statistic data for OCT4 levels at the different time points of the RA induced H9 differentiation. *, $P < 0.05$, by one way Anova using SPSS 17.0 software. Error bars represent standard error.

cotransfected 293 cells with FLAG–Vector (V), FLAG–DPF2 (WT) and FLAG–DPF2 (M) plasmids along with OCT4 plasmid in the presence of HA–Ub plasmid for 18 h. Then the cells were treated with MG132 for 6 h and subjected to denatured IP using an anti-OCT4 antibody. The following IB indicated that the denatured IP disrupted the interaction between OCT4 and DPF2 but did not affect the covalent conjugation

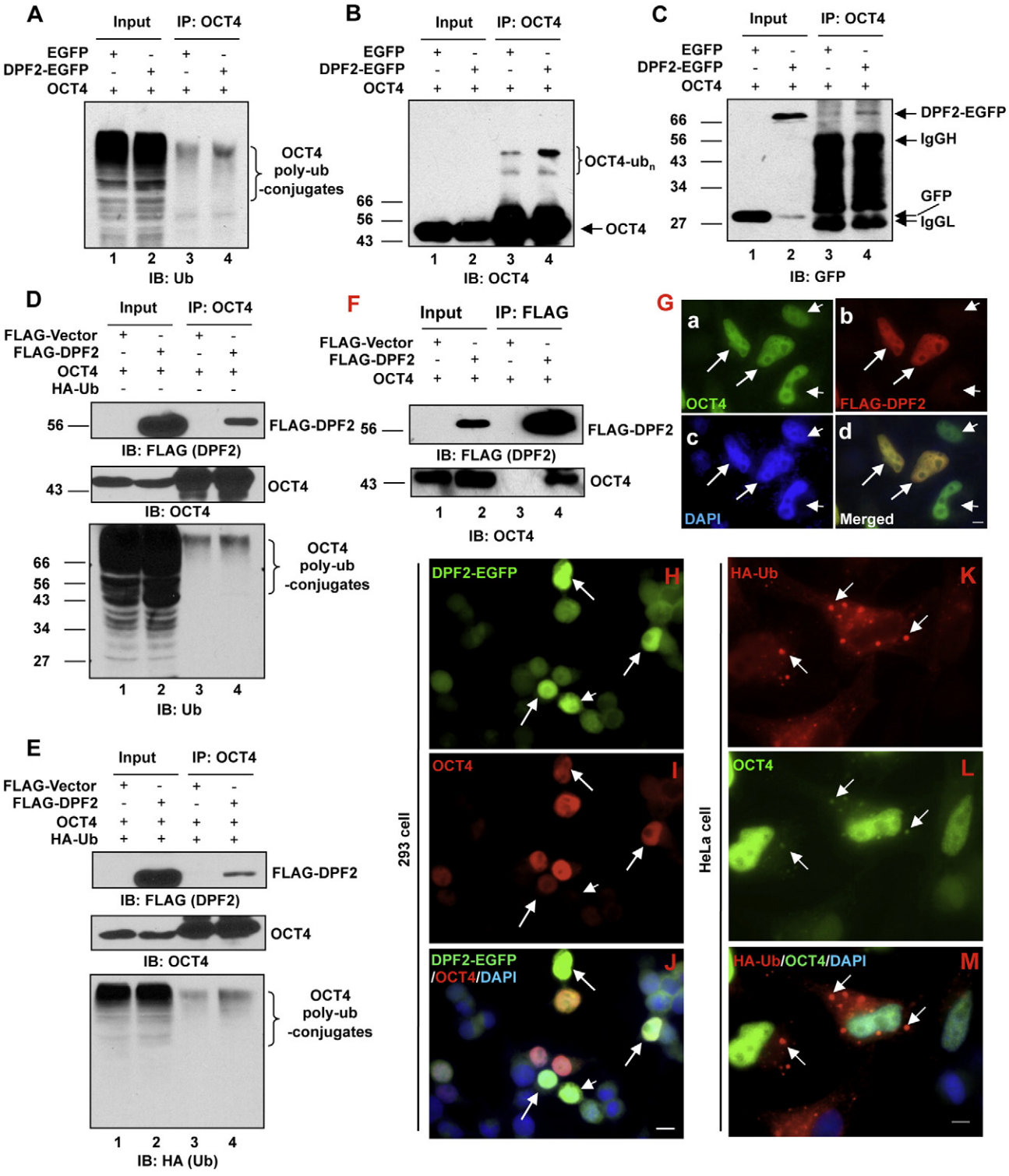

Fig. 5. Overexpression of DPF2 ubiquitinates ectopic OCT4 in 293 cells. A–C, 293 cells were transfected with EGFP–Vector, DPF2–EGFP along with OCT4. With the presence of MG132 for 6 h, cells were harvested and subject to IP assay with anti-OCT4 antibody followed by IB for Ub (A), OCT4 (B) and EGFP (C). IgGH, IgG heavy chain. IgGL, IgG light chain. D–F, 293 cells were transfected with FLAG–Vector, FLAG–DPF2 along with OCT4 with (E) or without (D) HA–Ub plasmids for 18 h. With the presence of MG132 for 6 h, cells were harvested and subject to IP assay with an anti-OCT4 antibody (D and E) and an anti-FLAG antibody (F), respectively, followed by IB for the indicated proteins. G, HeLa cells transfected by FLAG–DPF2 and OCT4 plasmids were subjected to IF assay with anti-OCT4 (a and d, green) and a Cy3-conjugated anti-FLAG antibodies (b and d, red). The nuclei were counterstained by DAPI. Bar = 5 μm. H–J, 293 cells transfected by DPF2–EGFP and OCT4 plasmids were subjected to fluorescence assay (H and J, green) and IF assay with anti-OCT4 antibody (I and I, red). The nuclei were counterstained by DAPI. Bar = 5 μm. K–M, HeLa cells transfected by FLAG–DPF2 and OCT4 along with HA–Ub plasmids were subjected to IF assay with anti-HA (K and M, red) and anti-OCT4 antibodies (L and M, green). The nuclei were counterstained by DAPI. Bar = 5 μm.

between Ub and OCT4 (Fig. 6G–H). Wild-type (Fig. 6H, lane 2), but not the PHD2 mutant (Fig. 6H, lane 3) form of DPF2 increased OCT4 ubiquitination. We also cotranfected 293 cells with FLAG–DPF2(WT)and FLAG–DPF2(M) along with OCT4 plasmids. IP assay in native condition using anti-OCT4 anti-body followed by IB with indicated antibodies was performed. The results showed that both wild type and PHD2 mutant

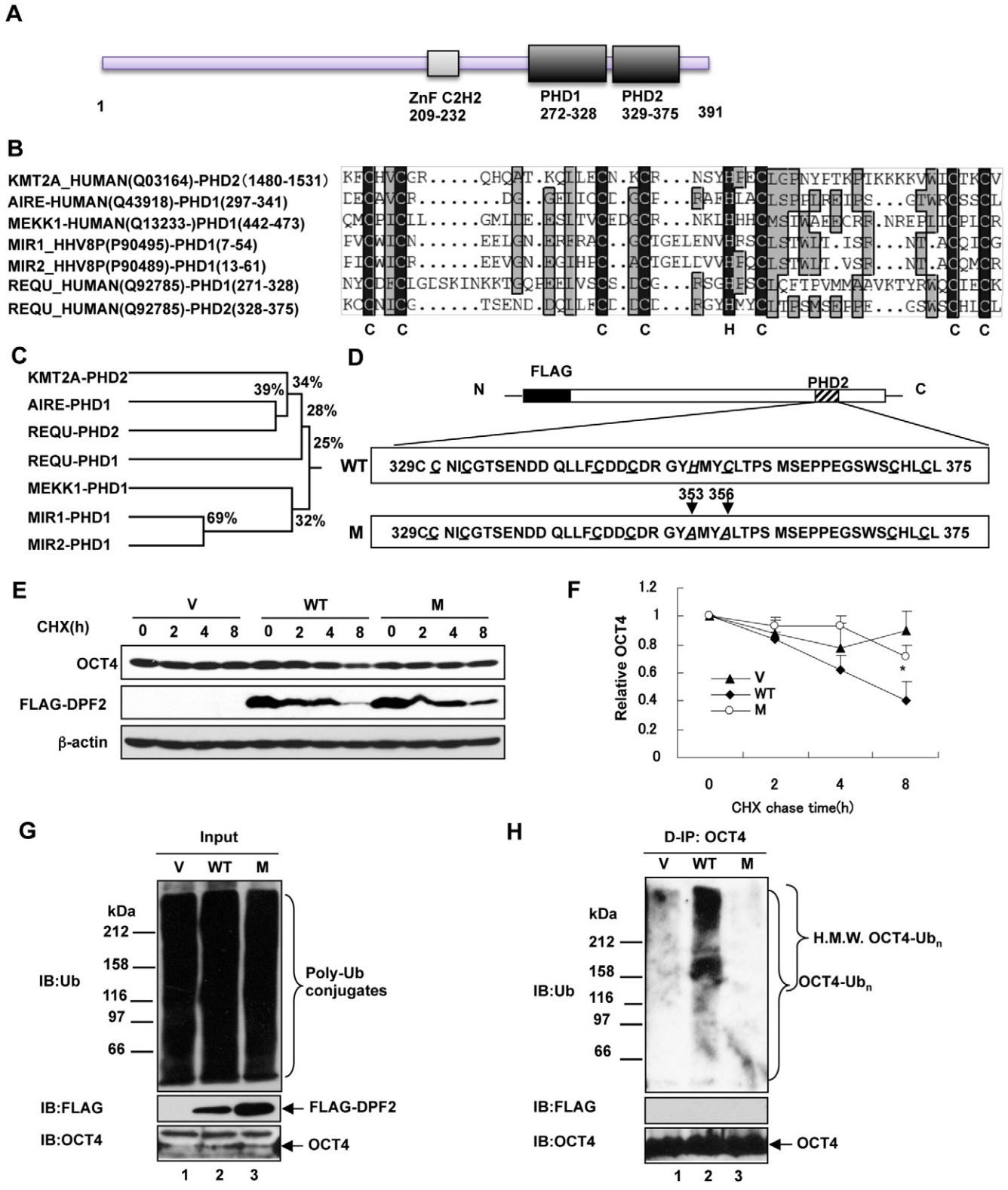

Fig. 6. The second PHD finger of DPF2 is involved in ubiquitination and degradation of OCT4. A, Schematic representation of domains within DPF2 (391 amino acids). A ZnF C2H2 domain, PHD1 (272–328) and PHD2 (279–375) fingers are shown. B, The PHD1 and PHD2 domains of DPF2 show homology with the PHD domains from other proteins showing E3 ubiquitin ligase activity. The Uniprot/Ensembl sequence identifier (ID)/accession number (ACC) of each protein is shown. C, homology tree and scores of PHD domains from DPF2 and other proteins showing E3 ubiquitinligase activity. D, Schematic representation of wild type (WT) PHD2 finger of human DPF2 and mutation (M) in PHD2 finger. E, 293 cells were transfected with FLAG–Vector (V), FLAG–DPF2 (WT) and FLAG–DPF2 (M) along with OCT4. A chase time assay was performed and cells were then harvested and lysed in NP-40 lysis buffer followed by SDS-PAGE and IB. F, data from 4 independent experiments were quantified based on the density of OCT4 bands. *, $P < 0.05$ compared to the vector and mutant DPF2, by independent sample T-test using SPSS 17.0 software. Error bars represent standard error. CHX, cycloheximide. G and H, 293 cells were transfected with FLAG–Vector (V), FLAG–DPF2 (WT) and FLAG–DPF2 (M) along with OCT4. Then the cells were subjected to denature-IP assay with anti-OCT4 antibody followed by IB for indicated proteins. D-IP, IP under denaturing conditions. H.M.W, high molecular weight.

DPF2 interact with OCT4. PHD2 mutant DPF2 decreased the OCT4 ubiquitination induced by wild type DPF2 (Fig. S3).

These results suggest that DPF2 contributes to ubiquitination and degradation of OCT4 in a PHD2-dependent manner.

3.7. DPF2 assembles mainly K48-linked ubiquitination of OCT4

The K linkage of Ub determines substrate fate [18]. Therefore, we examined which K residue (or residues) in the Ub molecule might be

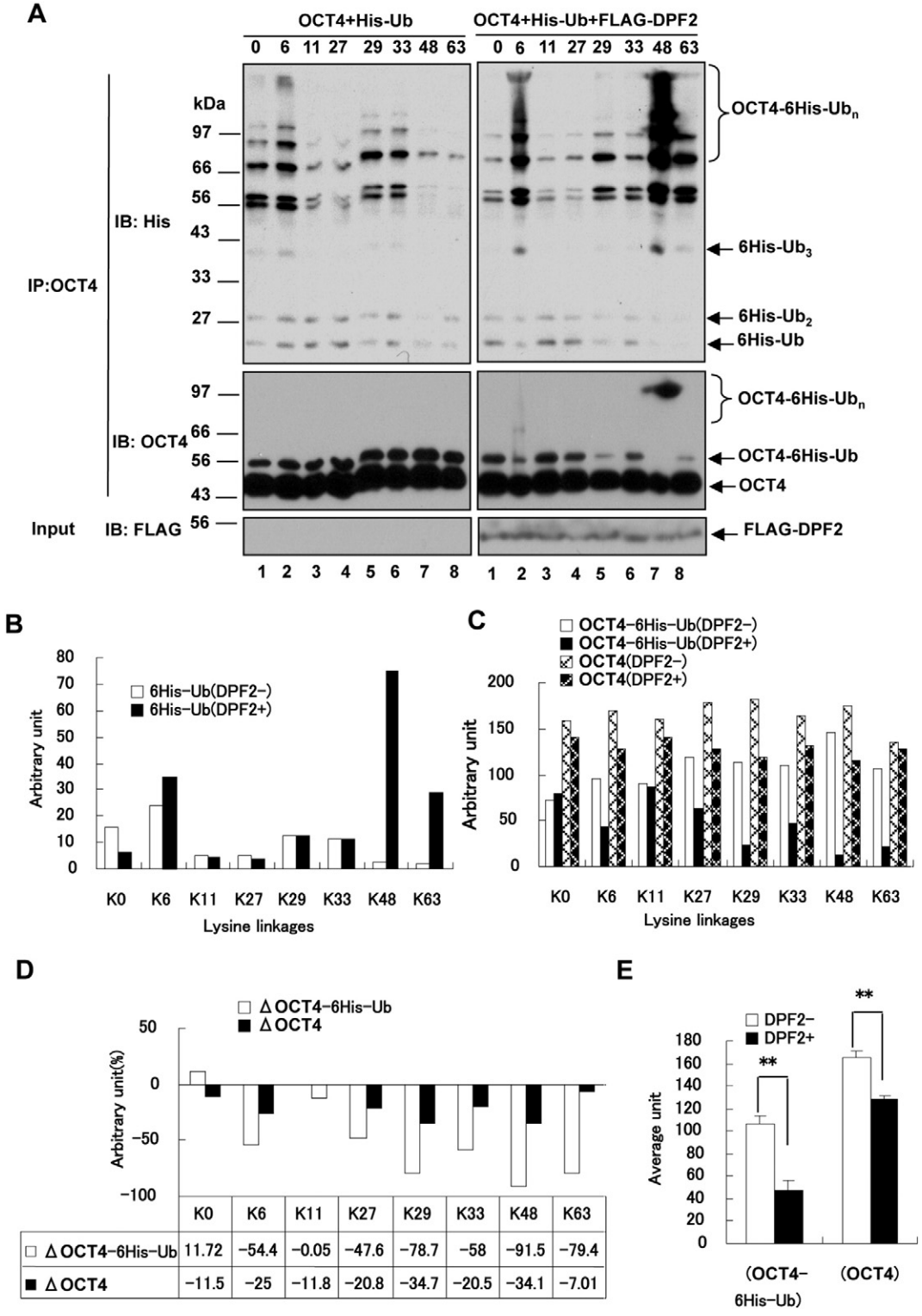

	K0	K6	K11	K27	K29	K33	K48	K63
□ ΔOCT4-6His-Ub	11.72	−54.4	−0.05	−47.6	−78.7	−58	−91.5	−79.4
■ ΔOCT4	−11.5	−25	−11.8	−20.8	−34.7	−20.5	−34.1	−7.01

Fig. 7. K48-linked ubiquitination of OCT4 by DPF2. A, 293 cells were transfected with OCT4 and one of the 6His-tagged mutant Ubs, as indicated, and either with or without FLAG–DPF2 (WT). At 18–20 h after transfection, cells were exposed to 20 μM MG132 for 6 h. Cells were then lysed and the lysates were subjected to IP with an OCT4 antibody followed by IB for the indicated proteins. B and C, quantification of OCT4 and OCT4–6His–Ub species as well as total 6His–Ub species coprecipitated with OCT4 for each lane in Fig. 6A. D, change in the density of OCT4 (ΔOCT4) and OCT4–6His–Ub (ΔOCT4–6His–Ub) as well as 6His–Ub species (Δ6His–Ub) in each lane was calculated and shown. E, statistic data for the average unit of OCT4 species and 6His–Ub species from 8 lanes. **, $P < 0.01$, by independent sample T-test using SPSS 17.0 software. Error bars represent standard error.

involved in the induction of poly-ubiquitin chains on OCT4 by DPF2. 293 cells were transfected with plasmids encoding OCT4 and a His-tagged Ub mutant without Ks (K0), or Ub mutants with a single K, with or without the presence of FLAG–DPF2 plasmids. Transfected cells were harvested and subjected to IP with an anti-OCT4 antibody, followed by IB for the indicated proteins. Bands representing mono-ubiquitinated OCT4 or OCT4–6His–Ub were detected (Fig. 7A, middle panels). Quantification of OCT4 species, including monomeric OCT4, OCT4–6His–Ub, and total 6His–Ub species coprecipitated with OCT4, was performed according to the density of related bands in Fig. 7A (Fig. 7B and C). The density change of the OCT4 species and 6His–Ub species, with (DPF2 +) or without (DPF2 −) DPF2, was calculated and shown, respectively (Fig. 7D and E).

Results indicated that poly-ubiquitinated OCT4 was detected even in the absence of DPF2, possibly generated by endogenous E3s for OCT4 (Fig. 7A, left panels). The expression of DPF2 enhanced the poly-ubiquitination of OCT4 in the presence of Ub–K6, Ub–K48 and Ub–K63, but not Ub–K0, Ub–K11, Ub–K27 and Ub–K29, suggesting that DPF2 may preferentially assemble poly-ubiquitin chains on OCT4 through K6, K48 and K63 linkages, of which K48 linkage is more efficient (Fig. 7A, right panels, lane 2, 7 and 8; Fig. 7B and D). Notably, while levels of monomeric OCT4 were down-regulated in the presence of Ub–K6 and Ub–K48 by DPF2, level of monomeric OCT4 in the presence of Ub–K63 was almost not changed (Fig. 7C). Actually, the average levels of OCT4 and mono-ubiquitinated OCT4 were down-regulated significantly (Fig. 7E). These results suggest that ubiquitination and degradation of OCT4 by DPF2 mainly depends on Ub–K48 residue.

3.8. Nuclear distribution of ectopic DPF2 and OCT4

Although OCT4 is expressed mainly in ESCs, subcellular localization of OCT4 has been studied using HeLa cell by several groups [16,17,57]. In our study, expression of ectopic OCT4 alone in HeLa cells resulted in diffusive distribution in nuclei (Fig. 8A–D). However, coexpression of FLAG–DPF2 (WT) and OCT4 formed a non-diffusive structure (Fig. 8E–H), in which DPF2 and OCT4 colocalized well, and also with DNA, as revealed by DAPI staining (Fig. 8E–H, arrows). Data employed more cells showed that while OCT4 alone was diffusive in nuclei (Fig. S4, A2, B2 and D2, arrowheads), OCT4 was non-diffusive in nuclei coexpressed robust DPF2 and OCT4 (Fig. S4, A1, B1 and D1, arrows). Moreover, with (Fig. 8E–H) or without (Fig. 8A–D) the presence of wild type DPF2, distribution of DAPI signals were similar with that of OCT4, which can also be identified in Fig. S4 (E–H and I–L, triangles).

We next asked whether the PHD2 of DPF2 is involved in regulating OCT4 sub-nuclear distribution. We transfected HeLa cells with plasmids encoding FLAG–DPF2 (M) (Fig. 8I and L, red) along with OCT4 plasmid (Fig. 8J and L, green). IF assay revealed that DPF2 (M) and OCT4 co-aggregates in nuclei (Fig. 8I, J and L, arrows). However, the aggregates are negative for DAPI staining (Fig. 8I, J and L, arrowheads). Data employed more cells showed that while OCT4 alone is diffusive in nuclei (Fig. S5, A2, B2 and D2, arrowheads), some of OCT4 signals co-aggregated with mutant DPF2 in nuclei double positive for mutant DPF2 and OCT4 (Fig. S5, A1, B1 and D1, arrows). Moreover, distribution of DNA signals in nuclei only positive for OCT4 was different with that of nuclei double positive for mutant DPF2 and OCT4 (Fig. S5, E–H, arrows). Through IP analysis, OCT4 coprecipitated with DPF2 (WT) and DPF2 (M) (Fig. 8M), suggesting the PHD2 mutation does not affect DPF2–OCT4 interaction. The schematic representation of DPF2 regulates OCT4 protein level and nuclear distribution is shown (Fig. 8N).

4. Discussion

In this study, we made several important novel observations: 1) DPF2 up-regulation is accompanied by OCT4 down-regulation during RA-induced H9 cell differentiation. 2) DPF2 interacts with OCT4 and acts as an E3 ligase. 3) *dpf2*/*DPF2* siRNAs increased OCT4 protein level in both P19 cells and H9 cells. 4) RA fails to downregulate OCT4 protein level in *DPF2*-knockdown H9 cells. 5) Overexpression of DPF2 changes the sub-nuclear localization of OCT4 and promotes ubiquitination and degradation of OCT4 in a PHD2-dependent manner. 6) Ubiquitination and degradation of OCT4 by DPF2 mainly depends on Ub–K48 residue.

At the beginning, we found that differentiated H9 cells expressed more DPF2 and that OCT4 down-regulation is accompanied by significant DPF2 up-regulation, not at the early stage but instead at a later stage in H9 cell differentiation induced by RA. In contrast, WWP2, an E3 that promotes OCT4 degradation in undifferentiated human ESCs, is quickly down-regulated after human ESC differentiation [24]. The primary role for WWP2 is assumed to be to regulate pluripotency rather than manipulate differentiation [60]. According to our data, DPF2 shRNA affects RA induced H9 cell differentiation and DPF2 catalyses ubiquitination and degradation of OCT4, implying that DPF2 might down-regulate OCT4 protein level through ubiquitination in hESC differentiation. Therefore, continued up-regulation of DPF2 during the prolonged differentiation period suggests that DPF2 may be involved in sustaining human ESC differentiation after the initiation of differentiation as a result of developmental or environmental signalling. This hypothesis is also supported by our finding that 293 cells and HeLa cells expressed higher levels of DPF2 than H9 cells.

The maintenance of stem cell self-renewal requires a precise level of OCT4 [4]. OCT4 manipulated above and below endogenous levels in human ESCs leads to divergent cell types [61]. Therefore, knockdown of DPF2 may induce differentiation of human ESCs through increasing OCT4 level. Interestingly, *DPF2* siRNA upregulates endogenous OCT4 level in H9 cells, but fails to increase protein level of NANOG, another pluripotent marker protein. It has been reported that NANOG is less stable than OCT4 and degradation of OCT4 is different from that of NANOG in stem cells [62]. Our finding here might also suggest the different stabilities between OCT4 and NANOG in human ESCs. These results imply that DPF2 may be a potential target for regulating OCT4 level and further ESC differentiation. OCT4 levels are also associated with tumour progression or bad diagnosis [63]. Overexpression of OCT4 enhanced whereas knockdown of OCT4 reduced liver cancer cell resistance to chemotherapeutic drugs [64]. DPF2 decreased the level of monomeric and monoubiquitinated OCT4 but increased poly-ubiquitination of OCT4. Mono-ubiquitination of OCT4 inhibits OCT4 transcription activity rather than targeting the protein for degradation [25]. DPF2 may regulate OCT4 activity through proteolytic and non-proteolytic pathways by regulating OCT4 mono-ubiquitination and/or poly-ubiquitination. Moreover, *in vitro* ubiquitnation assay indicates that DPF2 promotes OCT4 ubiquitnation. Thus, DPF2 might serve as a potential E3 that regulates OCT4 levels and function. How, when and where different OCT4 ubiquitination modifications and the resulting functional alterations are initiated warrants rigorous investigation in our future studies. PHD2 mutation of DPF2 forms aggregate-like structures with which

Fig. 8. Overexpression of DPF2 redistributes ectopic OCT4 in HeLa cells. A–H, HeLa cells grew on coverslips were transfected with FLAG–Vector (A–D) and FLAG–DPF2 (E–H) along with OCT4 plasmids. After 18 h, cells were fixed and subjected to IF assay for OCT4 (B, D, F and H, green) and DPF2 (E and H, red). Nuclei were counterstained by DAPI (C, D, G and H, blue). Bar = 5 μm. I–L, HeLa cells grew on coverslips were cotransfected with FLAG–DPF2 (M) and OCT4 plasmids. After 18 h, cells were fixed and subjected to fluorescence assay for OCT4 (J and L, green) and DPF2 (I and L, red). Nuclei were counterstained by DAPI (J and L, blue). Bar = 5 μm. M, 293 cells were transfected with FLAG–Vector (V), FLAG–DPF2 (WT) and FLAG–DPF2 (M) along with OCT4 plasmids for 18 h. After treatment with MG132 for 6 h, cells were lysed and lysates were subjected to IP assay with an anti-OCT4 antibody followed by IB for indicated proteins. N, schematic representation of DPF2 regulates OCT4 protein level and nuclear distribution. DPF2–OCT4 interaction might play role in OCT4–DNA binding, ubiquitination and degradation of OCT4. Ubiquitination of OCT4 might be mainly through Ub–K48 linkage. Mutation in PHD2 finger of DPF2 induces co-aggregation of mutant DPF2 and OCT4, which might decrease DNA binding, ubiquitination and degradation of OCT4.

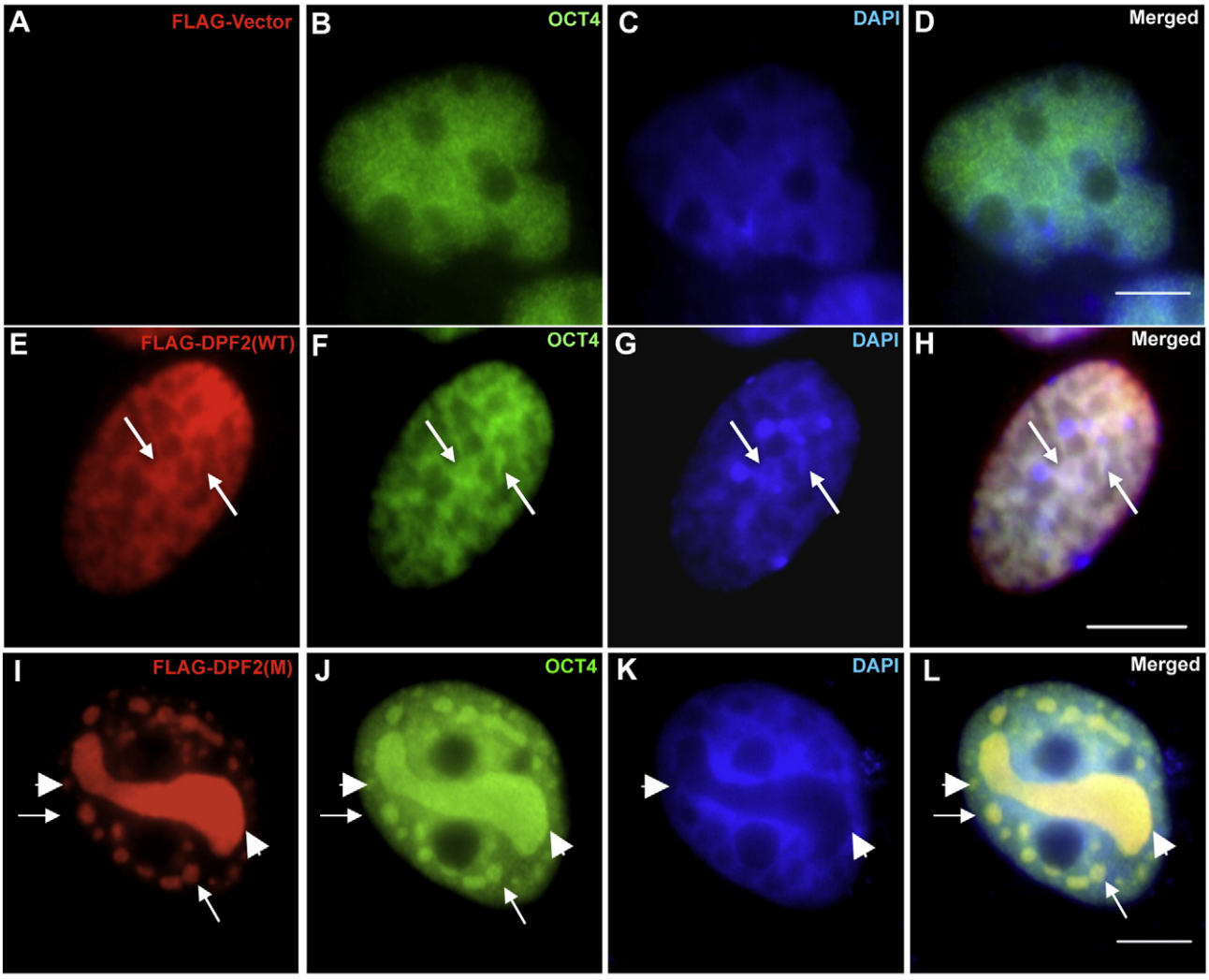
A
FLAG-Vector
B
OCT4
C
DAPI
D
Merged
E
FLAG-DPF2(WT)
F
OCT4
G
DAPI
H
Merged
I
FLAG-DPF2(M)
J
OCT4
K
DAPI
L
Merged

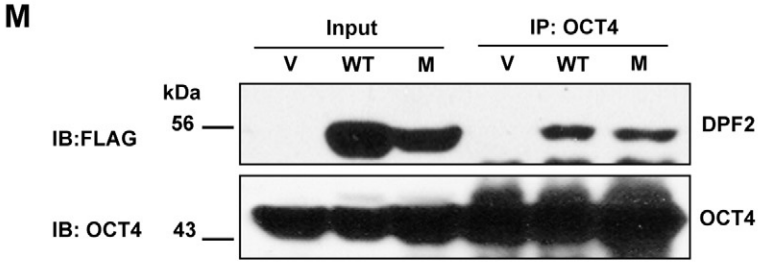
M
Input
IP: OCT4
V
WT
M
V
WT
M
kDa
56
IB:FLAG
DPF2
IB: OCT4
43
OCT4

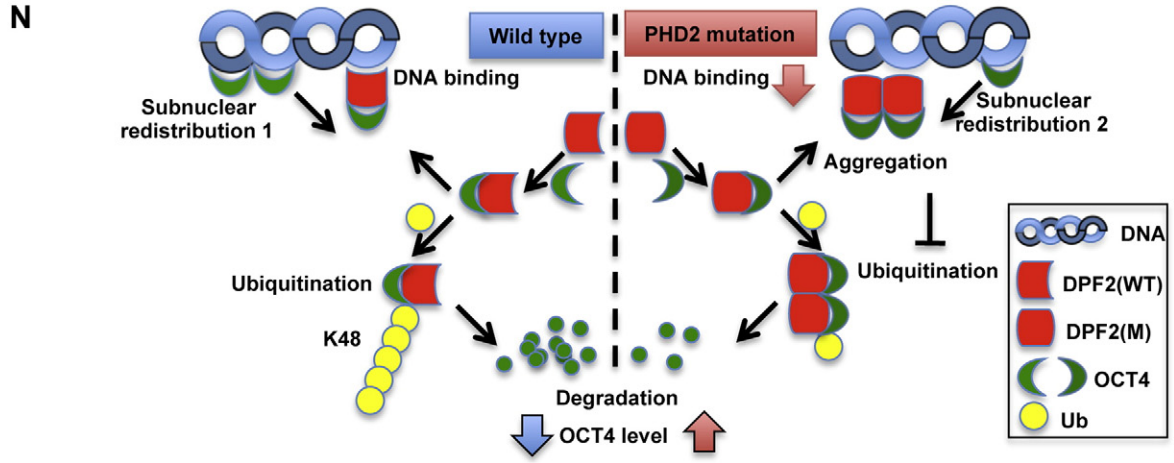
N
Wild type
PHD2 mutation
DNA binding
DNA binding
Subnuclear redistribution 1
Subnuclear redistribution 2
Aggregation
Ubiquitination
Ubiquitination
K48
Degradation
OCT4 level
DNA
DPF2(WT)
DPF2(M)
OCT4
Ub

OCT4 colocalized well (Figs. 7A–L and S5), which may affect the ubiquitination of OCT4 by not only DPF2 but also other E3s ligases. Thus, overexpressed PHD2 mutant DPF2 could be a dominant negative form of DPF2, which might inhibit endogenous ubiquitination of OCT4. For detecting ubiquitination of OCT4, MG132 treatment had been reported in several papers [24,25,65]. Interestingly, wwp2, a HECT-type E3 ubiquitin ligase, regulates ubiquitination and degradation of not only OCT4 but also itself [66]. We thus speculate proteasome inhibition mediated by MG132 may make it more promising for us to detect interaction proteins of OCT4 during CoIP and/or IP assays. The hypothesis is proved by our new finding that DPF2 is ubiquitinated *in vitro* (Fig. 3B) and its level is upregulated by MG132 in nuclei (see Fig. 3 in [59]). Previously, MG132 treatment increased OCT4 expression in undifferentiated cells [62,67]. Actually, the treatment of MG132 was performed for no more than 6 h just before harvesting the cells. Since MG132 can prevent degradation of a lot of proteins of which their levels are manipulated by UPS, including proteins involved in both pluripotency and differentiation [22], it thus might be *complex to examine if the treatment of MG132 for only 6 h could prevent OCT4 reduction during induced differentiation*. The benefit of MG132 treatment is to avoid protein degradation and get more proteins as possible as for following studies, in case some important proteins are degraded by UPS.

DPF2 assembled poly-ubiquitin chains on OCT4 through K6, K48 and K63 linkages, with K48-linkage is more efficient. K6-linked OCT4 ubiquitination was clearly identified by both anti-His and anti-OCT4 antibodies. However, K48 and K63-linked OCT4 ubiquitination was detected mainly using an anti-His antibody. Using an anti-OCT4 antibody, only high molecular weight bands were detected for the K48 linkage, suggesting DPF2 may generate mainly poly-ubiquitinated OCT4 speices with high molecular weight. Because different Ub lysine linkages may lead to different conformations of ubiquitinated substrates [68], we cannot exclude the possibility that these antibodies may not recognize the K48-linked ubiquitinated OCT4 species well. Notably, RNF2, a RING finger E3 that interacts with OCT4 and functions in maintaining stem cell pluripotency [23], also generates atypical mixed K6, K27 and K48 poly-ubiquitin linkages [69]. Another OCT4-interacting E3, WWP2, assembles K63 poly-ubiquitin linkage of OCT4 [24]. Hence, OCT4 ubiquitination *via* different lysine linkages is involved in regulating OCT4 function. Ubiquitination of a substrate *via* different lysines governs a variety of biological processes [68]. K48-linked ubiquitination targets a substrate protein for proteasomal degradation [70], whereas K63-linked ubiquitination contributes to the formation of protein aggregates [71]. Although K6-linked ubiquitination has a nonproteolytic effect on its target proteins [69], it also targets substrates for proteasomal degradation [72]. Actually, among all of the poly-ubiquitinated OCT4 induced by DPF2, more than a half was formed through Ub–K48 linkage, supporting our observation that proteasome inhibition increased OCT4 ubiquitination and DPF2 facilitated OCT4 degradation. However, the function of K6 and K63-linked ubiquitinated OCT4 remain to be elucidated.

As we know, OCT4 plays role in maintaining self renewal and pluripotency in ESCs. OCT4 also plays role in somatic cell reprogramming. Besides, OCT4 is involved in cancer development as a result of insufficient reprogramming [73] Therefore, understanding sub-cellular localization of OCT4 in both somatic cells and pluripotent stem cells is important. MG132 downregulated cytoplasmic DPF2 and induced accumulation of DPF2 in nuclei, in which OCT4 colocalized with accumulated DPF2(see Fig. 3 in ref. [59]). Because the right localization of OCT4 is required for its function in somatic cell reprogramming and ESC self renewal [16], the altered nuclear distribution of OCT4 by DPF2 in HeLa cells and H9 cells may more or less suggest a significance for reprogramming somatic cells into iPSCs and further, maintenance of self renewal of iPSCs. Regulation of OCT4 subnuclear distribution appears to require an intact PHD2 in DPF2. The PHD mutant form of DPF2, DPF2 (M), failed to redistribute OCT4, but retained its ability to interact with OCT4, leading to coaggregation of DPF2 (M) and OCT4 in the nuclei. Importantly, the DPF2 (M) and OCT4 aggregates are devoid of DNA, suggesting that the PHD may be required for DPF2 regulating OCT4 and DNA binding. In ESCs, DNA binding is required for OCT4 to associate with various promoter regions and to repress the transcription of various genes in one context while activate in another [1,74]. Another form of posttranslational modification, small ubiquitin-related modifier (SUMO) modification (sumoylation), was reported to enhance OCT4-DNA binding [75]. Whether ubiquitination of OCT4 might play a role in OCT4-DNA binding remains to be determined in our future studies.

Collectively, our findings presented here may expand an understanding of how OCT4 protein level and nuclear distribution is regulated and provide a potential target for manipulating OCT4 protein level.

Supplementary data to this article can be found online at http://dx.doi.org/10.1016/j.bbamcr.2015.09.029.

Conflict of interest statement

Here all authors disclose no conflict of interest.

Acknowledgements

This project was sponsored by a grant from the National Natural Science Foundation of China (31271159), a Maryland TEDCO grant (2007-MSCRFE-0139-01), a Technology Foundation for Selected Overseas Chinese Scholar Grant (2012 No. 13) from Anhui HRSS, a grant for scientific research of BSKY (XJ201105) from Anhui Medical University. We thank the help from Central Laboratory of Molecular and Cellular Biology, School of Basic Medical Sciences, Anhui Medical University. We thank Dr. Yun Qiu and Dr. Yihong Ye for providing plasmids.

References

[1] L.A. Boyer, T.I. Lee, M.F. Cole, S.E. Johnstone, S.S. Levine, J.P. Zucker, M.G. Guenther, R.M. Kumar, H.L. Murray, R.G. Jenner, D.K. Gifford, D.A. Melton, R. Jaenisch, R.A. Young, Core transcriptional regulatory circuitry in human embryonic stem cells, Cell 122 (2005) 947–956.
[2] Y. Babaie, R. Herwig, B. Greber, T.C. Brink, W. Wruck, D. Groth, H. Lehrach, T. Burdon, J. Adjaye, Analysis of Oct4-dependent transcriptional networks regulating self-renewal and pluripotency in human embryonic stem cells, Stem Cells 25 (2007) 500–510.
[3] M. Zuccotti, V. Merico, M. Bellone, F. Mulas, L. Sacchi, P. Rebuzzini, A. Prigione, C.A. Redi, R. Bellazzi, J. Adjaye, S. Garagna, Gatekeeper of pluripotency: a common Oct4 transcriptional network operates in mouse eggs and embryonic stem cells, BMC Genomics 12 (2011) 1–13.
[4] H. Niwa, J. Miyazaki, A.G. Smith, Quantitative expression of Oct-3/4 defines differentiation, dedifferentiation or self-renewal of ES cells, Nat. Genet. 24 (2000) 372–376.
[5] K. Takahashi, K. Tanabe, M. Ohnuki, M. Narita, T. Ichisaka, K. Tomoda, S. Yamanaka, Induction of pluripotent stem cells from adult human fibroblasts by defined factors, Cell 131 (2007) 861–872.
[6] J. Yu, M.A. Vodyanik, K. Smuga-Otto, J. Antosiewicz-Bourget, J.L. Frane, S. Tian, J. Nie, G.A. Jonsdottir, V. Ruotti, R. Stewart, I.I. Slukvin, J.A. Thomson, Induced pluripotent stem cell lines derived from human somatic cells, Science 318 (2007) 1917–1920.
[7] I.H. Park, R. Zhao, J.A. West, A. Yabuuchi, H. Huo, T.A. Ince, P.H. Lerou, M.W. Lensch, G.Q. Daley, Reprogramming of human somatic cells to pluripotency with defined factors, Nature 451 (2008) 141–146.
[8] J.B. Kim, V. Sebastiano, G. Wu, M.J. Arauzo-Bravo, P. Sasse, L. Gentile, K. Ko, D. Ruau, M. Ehrich, D. van den Boom, J. Meyer, K. Hubner, C. Bernemann, C. Ortmeier, M. Zenke, B.K. Fleischmann, H. Zaehres, H.R. Scholer, Oct4-induced pluripotency in adult neural stem cells, Cell 136 (2009) 411–419.
[9] Y. Li, Q. Zhang, X. Yin, W. Yang, Y. Du, P. Hou, J. Ge, C. Liu, W. Zhang, X. Zhang, Y. Wu, H. Li, K. Liu, C. Wu, Z. Song, Y. Zhao, Y. Shi, H. Deng, Generation of iPSCs from mouse fibroblasts with a single gene, Oct4, and small molecules, Cell Res. 21 (2011) 196–204.
[10] Y.A. Tang, C.H. Chen, H.S. Sun, C.P. Cheng, V.S. Tseng, H.S. Hsu, W.C. Su, W.W. Lai, Y.C. Wang, Global Oct4 target gene analysis reveals novel downstream PTEN and TNC genes required for drug-resistance and metastasis in lung cancer, Nucleic Acids Res. 43 (2015) 1593–1608.
[11] Y.D. Wang, N. Cai, X.L. Wu, H.Z. Cao, L.L. Xie, P.S. Zheng, OCT4 promotes tumorigenesis and inhibits apoptosis of cervical cancer cells by miR-125b/BAK1 pathway, Cell Death Dis. 4 (2013), e760.
[12] Y. Lu, H. Zhu, H. Shan, J. Lu, X. Chang, X. Li, X. Fan, S. Zhu, Y. Wang, Q. Guo, L. Wang, Y. Huang, M. Zhu, Z. Wang, Knockdown of Oct4 and Nanog expression inhibits the stemness of pancreatic cancer cells, Cancer Lett. 340 (2013) 113–123.
[13] S.H. Chiou, M.L. Wang, Y.T. Chou, C.J. Chen, C.F. Hong, W.J. Hsieh, H.T. Chang, Y.S. Chen, T.W. Lin, H.S. Hsu, C.W. Wu, Coexpression of Oct4 and Nanog enhances malignancy in lung adenocarcinoma by inducing cancer stem cell-like properties and epithelial-mesenchymal transdifferentiation, Cancer Res. 70 (2010) 10433–10444.

[14] F.Y. Al-Marzoqee, G. Khoder, H. Al-Awadhi, R. John, A. Beg, A. Vincze, F. Branicki, S.M. Karam, Upregulation and inhibition of the nuclear translocation of Oct4 during multistep gastric carcinogenesis, Int. J. Oncol. 41 (2012) 1733–1743.
[15] G. Karoubi, L. Cortes-Dericks, M. Gugger, D. Galetta, L. Spaggiari, R.A. Schmid, Atypical expression and distribution of embryonic stem cell marker, OCT4, in human lung adenocarcinoma, J. Surg. Oncol. 102 (2010) 689–698.
[16] M. Oka, T. Moriyama, M. Asally, K. Kawakami, Y. Yoneda, Differential role for transcription factor Oct4 nucleocytoplasmic dynamics in somatic cell reprogramming and self-renewal of embryonic stem cells, J. Biol. Chem. 288 (2013) 15085–15097.
[17] G. Pan, B. Qin, N. Liu, H.R. Scholer, D. Pei, Identification of a nuclear localization signal in OCT4 and generation of a dominant negative mutant by its ablation, J. Biol. Chem. 279 (2004) 37013–37020.
[18] A.M. Weissman, Themes and variations on ubiquitylation, Nat. Rev. Mol. Cell Biol. 2 (2001) 169–178.
[19] R. Layfield, J.R. Cavey, J. Lowe, Role of ubiquitin-mediated proteolysis in the pathogenesis of neurodegenerative disorders, Ageing Res. Rev. 2 (2003) 343–356.
[20] A. Hershko, A. Ciechanover, The ubiquitin system, Annu. Rev. Biochem. 67 (1998) 425–479.
[21] J.S. Thrower, L. Hoffman, M. Rechsteiner, C.M. Pickart, Recognition of the polyubiquitin proteolytic signal, EMBO J. 19 (2000) 94–102.
[22] C. Naujokat, T. Saric, Concise review: role and function of the ubiquitin-proteasome system in mammalian stem and progenitor cells, Stem Cells 25 (2007) 2408–2418.
[23] M. Endoh, T.A. Endo, T. Endoh, Y. Fujimura, O. Ohara, T. Toyoda, A.P. Otte, M. Okano, N. Brockdorff, M. Vidal, H. Koseki, Polycomb group proteins ring1a/B are functionally linked to the core transcriptional regulatory circuitry to maintain ES cell identity, Development 135 (2008) 1513–1524.
[24] H. Xu, W. Wang, C. Li, H. Yu, A. Yang, B. Wang, Y. Jin, WWP2 promotes degradation of transcription factor OCT4 in human embryonic stem cells, Cell Res. 19 (2009) 561–573.
[25] H.M. Xu, B. Liao, Q.J. Zhang, B.B. Wang, H. Li, X.M. Zhong, H.Z. Sheng, Y.X. Zhao, Y.M. Zhao, Y. Jin, Wwp2, an E3 ubiquitin ligase that targets transcription factor Oct-4 for ubiquitination, J. Biol. Chem. 279 (2004) 23495–23503.
[26] T. Geetha, R.S. Kenchappa, M.W. Wooten, B.D. Carter, TRAF6-mediated ubiquitination regulates nuclear translocation of NRIF, the p75 receptor interactor, EMBO J. 24 (2005) 3859–3868.
[27] J.P. Kruse, W. Gu, MSL2 promotes Mdm2-independent cytoplasmic localization of p53, J. Biol. Chem. 284 (2009) 3250–3263.
[28] M.B. Metzger, V.A. Hristova, A.M. Weissman, HECT and RING finger families of E3 ubiquitin ligases at a glance, J. Cell Sci. 125 (2012) 531–537.
[29] M. Scheffner, S. Kumar, Mammalian HECT ubiquitin-protein ligases: biological and pathophysiological aspects, Biochim. Biophys. Acta 1843 (2014) 61–74.
[30] M. Pardo, B. Lang, L. Yu, H. Prosser, A. Bradley, M.M. Babu, J. Choudhary, An expanded Oct4 interaction network: implications for stem cell biology, development, and disease, Cell Stem Cell 6 (2010) 382–395.
[31] J. Wang, S. Rao, J. Chu, X. Shen, D.N. Levasseur, T.W. Theunissen, S.H. Orkin, A protein interaction network for pluripotency of embryonic stem cells, Nature 444 (2006) 364–368.
[32] D.L. van den Berg, T. Snoek, N.P. Mullin, A. Yates, K. Bezstarosti, J. Demmers, I. Chambers, R.A. Poot, An Oct4-centered protein interaction network in embryonic stem cells, Cell Stem Cell 6 (2010) 369–381.
[33] T.G. Gabig, P.L. Mantel, R. Rosli, C.D. Crean, Requiem: a novel zinc finger gene essential for apoptosis in myeloid cells, J. Biol. Chem. 269 (1994) 29515–29519.
[34] Y. Lim, V.X. Seah, A. Mantalaris, M.G. Yap, D.C. Wong, Elucidating the role of requiem in the growth and death of Chinese hamster ovary cells, Apoptosis 15 (2010) 450–462.
[35] T. Tando, A. Ishizaka, H. Watanabe, T. Ito, S. Iida, T. Haraguchi, T. Mizutani, T. Izumi, T. Isobe, T. Akiyama, J. Inoue, H. Iba, Requiem protein links RelB/p52 and the Brm-type SWI/SNF complex in a noncanonical NF-kappaB pathway, J. Biol. Chem. 285 (2010) 21951–21960.
[36] C. Tallant, E. Valentini, O. Fedorov, L. Overvoorde, F.M. Ferguson, P. Filippakopoulos, D.I. Svergun, S. Knapp, A. Ciulli, Molecular basis of histone tail recognition by human TIP5 PHD finger and bromodomain of the chromatin remodeling complex NoRC, Structure 23 (2015) 80–92.
[37] J.G. Rack, T. Lutter, G.E. Kjaereng Bjerga, C. Guder, C. Ehrhardt, S. Varv, M. Ziegler, R. Aasland, The PHD finger of p300 influences its ability to acetylate histone and non-histone targets, J. Mol. Biol. 426 (2014) 3960–3972.
[38] M. Bienz, The PHD finger, a nuclear protein-interaction domain, Trends Biochem. Sci. 31 (2006) 35–40.
[39] J. Wang, A.G. Muntean, L. Wu, J.L. Hess, A subset of mixed lineage leukemia proteins has plant homeodomain (PHD)-mediated E3 ligase activity, J. Biol. Chem. 287 (2012) 43410–43416.
[40] X. Qiu, B.E. Dul, N.C. Walworth, Activity of a C-terminal plant homeodomain (PHD) of Msc1 is essential for function, J. Biol. Chem. 285 (2010) 36828–36835.
[41] D. Uchida, S. Hatakeyama, A. Matsushima, H. Han, S. Ishido, H. Hotta, J. Kudoh, N. Shimizu, V. Doucas, K.I. Nakayama, N. Kuroda, M. Matsumoto, AIRE functions as an E3 ubiquitin ligase, J. Exp. Med. 199 (2004) 167–172.
[42] Z. Lu, S. Xu, C. Joazeiro, M.H. Cobb, T. Hunter, The PHD domain of MEKK1 acts as an E3 ubiquitin ligase and mediates ubiquitination and degradation of ERK1/2, Mol. Cell 9 (2002) 945–956.
[43] L. Coscoy, D.J. Sanchez, D. Ganem, A novel class of herpesvirus-encoded membrane-bound E3 ubiquitin ligases regulates endocytosis of proteins involved in immune recognition, J. Cell Biol. 155 (2001) 1265–1273.
[44] E.W. Hewitt, L. Duncan, D. Mufti, J. Baker, P.G. Stevenson, P.J. Lehner, Ubiquitylation of MHC class I by the K3 viral protein signals internalization and TSG101-dependent degradation, EMBO J. 21 (2002) 2418–2429.
[45] X. Chen, Z. Du, W. Shi, C. Wang, Y. Yang, F. Wang, Y. Yao, K. He, A. Hao, 2-Bromopalmitate modulates neuronal differentiation through the regulation of histone acetylation, Stem Cell Res. 12 (2014) 481–491.
[46] A. Apostolou, Y. Shen, Y. Liang, J. Luo, S. Fang, Armet, a UPR-upregulated protein, inhibits cell proliferation and ER stress-induced cell death, Exp. Cell Res. 314 (2008) 2454–2467.
[47] H. Yang, C. Liu, Y. Zhong, S. Luo, M.J. Monteiro, S. Fang, Huntingtin interacts with the cue domain of gp78 and inhibits gp78 binding to ubiquitin and p97/VCP, PLoS One 5 (2010), e8905.
[48] L. Liu, C. Liu, Y. Zhong, A. Apostolou, S. Fang, ER stress response during the differentiation of H9 cells induced by retinoic acid, Biochem. Biophys. Res. Commun. 417 (2012) 738–743.
[49] C. Liu, Y. Sun, J. Arnold, B. Lu, S. Guo, Synergistic contribution of SMAD signaling blockade and high localized cell density in the differentiation of neuroectoderm from H9 cells, Biochem. Biophys. Res. Commun. 452 (2014) 895–900.
[50] S. Dan, B. Kang, X. Duan, Y.-J. Wang, A cell-free system toward deciphering the post-translational modification barcodes of Oct4 in different cellular contexts, Biochem. Biophys. Res. Commun. 456 (2015) 714–720.
[51] S. Fang, M. Ferrone, C. Yang, J.P. Jensen, S. Tiwari, A.M. Weissman, The tumor autocrine motility factor receptor, gp78, is a ubiquitin protein ligase implicated in degradation from the endoplasmic reticulum, Proc. Natl. Acad. Sci. U. S. A. 98 (2001) 14422–14427.
[52] J. Fan, H. Ren, N. Jia, E. Fei, T. Zhou, P. Jiang, M. Wu, G. Wang, DJ-1 decreases Bax expression through repressing p53 transcriptional activity, J. Biol. Chem. 283 (2008) 4022–4030.
[53] Z.W. Du, S.C. Zhang, Lentiviral vector-mediated transgenesis in human embryonic stem cells, Methods Mol. Biol. 614 (2010) 127–134.
[54] N. Matsuda, T. Suzuki, K. Tanaka, A. Nakano, Rma1, a novel type of RING finger protein conserved from Arabidopsis to human, is a membrane-bound ubiquitin ligase, J. Cell Sci. 114 (2001) 1949–1957.
[55] R. Paolini, R. Molfetta, M. Piccoli, L. Frati, A. Santoni, Ubiquitination and degradation of Syk and ZAP-70 protein tyrosine kinases in human NK cells upon CD16 engagement, Proc. Natl. Acad. Sci. U. S. A. 98 (2001) 9611–9616.
[56] P. Gupta, P.C. Ho, M.M. Huq, S.G. Ha, S.W. Park, A.A. Khan, N.P. Tsai, L.N. Wei, Retinoic acid-stimulated sequential phosphorylation, PML recruitment, and SUMOylation of nuclear receptor TR2 to suppress Oct4 expression, Proc. Natl. Acad. Sci. U. S. A. 105 (2008) 11424–11429.
[57] R. Spelat, F. Ferro, F. Curcio, Serine 111 phosphorylation regulates OCT4A protein subcellular distribution and degradation, J. Biol. Chem. 287 (2012) 38279–38288.
[58] P. van der Stoop, E.A. Boutsma, D. Hulsman, S. Noback, M. Heimerikx, R.M. Kerkhoven, J.W. Voncken, L.F. Wessels, M. van Lohuizen, Ubiquitin E3 ligase Ring1b/Rnf2 of polycomb repressive complex 1 contributes to stable maintenance of mouse embryonic stem cells, PLoS One 3 (2008), e2235.
[59] C. Liu, D. Zhang, Y. Shen, X. Tao, L. Liu, Y. Zhong, S. Fang, Data in support of DPF2 regulates OCT4 protein level and nuclear distribution, Data Brief (2015) (submitted for publication).
[60] R.T. Wagner, A.J. Cooney, OCT4: less is more, Cell Res. 19 (2009) 527–528.
[61] R.T. Rodriguez, J.M. Velkey, C. Lutzko, R. Seerke, D.B. Kohn, K.S. O'Shea, M.T. Firpo, Manipulation of OCT4 levels in human embryonic stem cells results in induction of differential cell types, Exp. Biol. Med. (Maywood) 232 (2007) 1368–1380.
[62] Y. Yao, Y. Lu, W.C. Chen, Y. Jiang, T. Cheng, Y. Ma, L. Lu, W. Dai, Cobalt and nickel stabilize stem cell transcription factor OCT4 through modulating its sumoylation and ubiquitination, PLoS One 9 (2014), e86620.
[63] M. Schoenhals, A. Kassambara, J. De Vos, D. Hose, J. Moreaux, B. Klein, Embryonic stem cell markers expression in cancers, Biochem. Biophys. Res. Commun. 383 (2009) 157–162.
[64] X.Q. Wang, W.M. Ongkeko, L. Chen, Z.F. Yang, P. Lu, K.K. Chen, J.P. Lopez, R.T. Poon, S.T. Fan, Octamer 4 (Oct4) mediates chemotherapeutic drug resistance in liver cancer cells through a potential Oct4–AKT–ATP–binding cassette G2 pathway, Hepatology 52 (2010) 528–539.
[65] B. Liao, X. Zhong, H. Xu, F. Xiao, Z. Fang, J. Gu, Y. Chen, Y. Zhao, Y. Jin, Itch, an E3 ligase of Oct4, is required for embryonic stem cell self-renewal and pluripotency induction, J. Cell. Physiol. 228 (2013) 1443–1451.
[66] B. Liao, Y. Jin, Wwp2 mediates Oct4 ubiquitination and its own auto-ubiquitination in a dosage-dependent manner, Cell Res. 20 (2010) 332–344.
[67] J.P. Saxe, A. Tomilin, H.R. Scholer, K. Plath, J. Huang, Post-translational regulation of Oct4 transcriptional activity, PLoS One 4 (2009), e4467.
[68] W. Li, Y. Ye, Polyubiquitin chains: functions, structures, and mechanisms, Cell. Mol. Life Sci. 65 (2008) 2397–2406.
[69] R. Ben-Saadon, D. Zaaroor, T. Ziv, A. Ciechanover, The polycomb protein Ring1B generates self atypical mixed ubiquitin chains required for its in vitro histone H2A ligase activity, Mol. Cell 24 (2006) 701–711.
[70] K. Haglund, I. Dikic, Ubiquitylation and cell signaling, EMBO J. 24 (2005) 3353–3359.
[71] C. Liu, E. Fei, N. Jia, H. Wang, R. Tao, A. Iwata, N. Nukina, J. Zhou, G. Wang, Assembly of lysine 63-linked ubiquitin conjugates by phosphorylated alpha-synuclein implies Lewy body biogenesis, J. Biol. Chem. 282 (2007) 14558–14566.
[72] P. Xu, D.M. Duong, N.T. Seyfried, D. Cheng, Y. Xie, J. Robert, J. Rush, M. Hochstrasser, D. Finley, J. Peng, Quantitative proteomics reveals the function of unconventional ubiquitin chains in proteasomal degradation, Cell 137 (2009) 133–145.
[73] K. Ohnishi, K. Semi, T. Yamamoto, M. Shimizu, A. Tanaka, K. Mitsunaga, K. Okita, K. Osafune, Y. Arioka, T. Maeda, H. Soejima, H. Moriwaki, S. Yamanaka, K. Woltjen, Y. Yamada, Premature termination of reprogramming in vivo leads to cancer development through altered epigenetic regulation, Cell 156 (2014) 663–677.
[74] H.R. Scholer, S. Ruppert, N. Suzuki, K. Chowdhury, P. Gruss, New type of POU domain in germ line-specific protein Oct-4, Nature 344 (1990) 435–439.
[75] F. Wei, H.R. Scholer, M.L. Atchison, Sumoylation of Oct4 enhances its stability, DNA binding, and transactivation, J. Biol. Chem. 282 (2007) 21551–21560.